PULSE GENERATION IN ERBIUM-DOPED FIBER LASER USING A PASSIVE TECHNIQUE

MUHAMAD BURHAN SHAH BIN SABRAN

INSTITUTE OF GRADUATE STUDIES
UNIVERSITY OF MALAYA
KUALA LUMPUR

2016

PULSE GENERATION IN ERBIUM-DOPED FIBER LASER USING A PASSIVE TECHNIQUE

MUHAMAD BURHAN SHAH BIN SABRAN

DESSERTATION SUBMITTED IN FULFILMENT OF THE REQUIREMENT FOR THE DEGREE OF MASTER OF PHILOSOPHY

INSTITUTE OF GRADUATE STUDIES
UNIVERSITY OF MALAYA
KUALA LUMPUR

2016

UNIVERSITY OF MALAYA

ORIGINAL LITERARY WORK DECLARATION

Name of Candidate:MUHAMAD BURHAN SHAH BIN SABRAN

Registration/Matric No:HGG130002

Name of Degree:MASTER OF PHILOSOPHY

Title of Project Paper/Research Report/Dissertation/Thesis ("this Work"):

PULSE GENERATION IN ERBIUM-DOPED FIBER LASER USING A PASSIVE TECHNIQUE

Field of Study:PHOTONIC ENGINEERING

I do solemnly and sincerely declare that:

(1) I am the sole author/writer of this Work;
(2) This Work is original;
(3) Any use of any work in which copyright exists was done by way of fair dealing and for permitted purposes and any excerpt or extract from, or reference to or reproduction of any copyright work has been disclosed expressly and sufficiently and the title of the Work and its authorship have been acknowledged in this Work;
(4) I do not have any actual knowledge nor do I ought reasonably to know that the making of this work constitutes an infringement of any copyright work;
(5) I hereby assign all and every rights in the copyright to this Work to the University of Malaya ("UM"), who henceforth shall be owner of the copyright in this Work and that any reproduction or use in any form or by any means whatsoever is prohibited without the written consent of UM having been first had and obtained;
(6) I am fully aware that if in the course of making this Work I have infringed any copyright whether intentionally or otherwise, I may be subject to legal action or any other action as may be determined by UM.

Candidate's Signature Date:

Subscribed and solemnly declared before,

Witness's Signature Date:

Name:

Designation:

ABSTRACT

Various new pulsed fiber lasers operating in single-wavelength and dual-wavelength modes are proposed and demonstrated using a low cost and simple approach. At first, a stable passive Q-switched fiber laser operating at 1543.5 nm is demonstrated using a double-clad Erbium-Ytterbium co-doped fiber (EYDF) as the gain medium in conjunction with nonlinear polarization rotation (NPR) technique. Polarization dependent isolator is used in conjunction with a highly nonlinear EYDF to induce intensity dependent loss in a sufficiently-high loss ring cavity to achieve Q-switched operation. At 980 nm multimode pump power of 500 mW, the EYDF laser (EYDFL) generates an optical pulse train with a repetition rate of 46.95 kHz, pulse width of 5.3 μs and pulse energy of 75.6 nJ. A dual-wavelength EYDFL is also demonstrated using the similar NPR technique. Besides, the NPR, graphene oxide (GO) could also be used as a saturable absorber (SA) in fiber laser cavity for pulse generation. In this work, two different Q-switched Erbium-doped fiber lasers (EDFLs) are demonstrated using a GO paper as a SA. A stable and self-starting Q-switched operation was achieved at 1534.4 nm by using a 0.8 m long Erbium-doped fiber (EDF) as gain medium. The pulse repetition rate changes from 14.3 to 31.5 kHz while the corresponding pulse width decreases from 32.8 to 13.8 μs as the pump power is increased from 22.0 to 50.5 mW. A narrow spacing dual-wavelength Q-switched EDFL can also be realized by including a photonics crystal fiber and a tunable Bragg filter in the setup. Finally, a mode-locked EDFL is demonstrated by using the similar GO paper SA. A GO SA based mode-locked EDFL can be realized by using a 1.6 m long EDF in conjunction with 1480 nm pumping. The laser generates a soliton pulse train with a repetition rate of 15.62 MHz and pulse width of 870 fs. These results show that the proposed GO paper is a suitable SA component for generating both Q-switched and mode-locked EDFL operating in 1.5 micron wavelength region.

ABSTRAK

Pelbagai gentian laser berdenyut yang beroperasi di satu panjang gelombang dan dwi-panjang gelombang mod dan berasaskan penggunakan kos yang rendah dan mudah. Pada mulanya, gentian laser stabil pasif Q-switched beroperasi pada 1543.5 nm ditunjukkan menggunakan gentian optik terdop Erbium-Ytterbium (EYDF) sebagai aktif medium bersama-sama dengan teknik putaran polarisasi tak linear (NPR). Isolator mengikut polariti digunakan bersama dengan EYDF yang bersifat tak-linear untuk mendorong kesan keamatan modulasi yang cukup tinggi untuk mencapai operasi Q-switched. Pada kuasa pam 980 nm sebanyak 500 mW, laser EYDF (EYDFL) menjana deretan denyutan nadi dengan frekuensi 46.95 kHz, lebar denyut 5.3 μs dan tenaga nadi 75.6 nJ. EYDFL dengan dwi-panjang gelombang dapat juga dihasilkan menggunakan teknik NPR yang sama. Selain NPR, graphene oksida (GO) juga boleh digunakan sebagai penyerap tepu (SA) dalam laser caviti untuk penghasilan denyutan nadi. Dalam kerja ini, dua Q-switched laser juga dilaporkan menggunakanlaser berasaskan gentian optik terdop Erbium (EDFL) dan menggunakan kertas GO sebagai SA. Operasi Q-switched adalah stabil dengan panjang gelombang 1534.4 nm telah berjaya dihasilkan dengan menggunakan 0.8 m EDFsebagai medium aktif. Frekuensi bertambah dari 14.3 ke 31.5 kHz manakala lebar denyut berkurangan dari 32.8 ke 13.8 μs jika kuasa pam meningkat dari 22.0 ke 50.5 mW. EDFL dengan dwi-panjang gelombang dan bersifat Q-switched boleh dicapai dengan memasukkan serat kristal fotonik dan penapis Bragg dalam laser kaviti. Akhir sekali, mod locked EDFL juga dapat ditunjukkan dengan menggunakan kertas GO SA yang sama. Mod locked EDFL dapat dijana dengan menggunakan 1.6 m panjang EDF bersama 1480 nm pam. Laser ini menjana deretan denyut soliton dengan frekuensi 15.62 MHz dan lebar denyut 870 fs. Keputusan ini menunjukkan kertas GO dapat berfungsi sebagai komponen SA menjana kedua-dua Q-switched dan mod locked EDFL beroperasi di rantau panjang gelombang 1.5 mikron.

ACKNOWLEDGEMENTS

I would like to express my greatest gratitude to my supervisor Prof. Dr. Sulaiman Wadi Harun for their continuous guidance and patience towards my research development process. They have guided me strictly to make sure that I have produced my best effort. They had spent their valuable time with me to discuss any problems and issues faced by me.

My sincere appreciation goes to Prof. Dr. Harith Ahmad for helping me get started in the lab and gave me many illuminating thoughts and discussion and helped me in my research.

In addition, I would like to greatly thank my family for their endless love and continuous support, especially my wife Nor Hafizah Binti Muzaiyin who always care for my study and tried to be patient for my absence, thanks to them for understanding and giving me this chance to complete my research .

Last but not least, I would like to take this opportunity and thank all my friends in who gave me their words of encouragement and motivated me to finish my research.

Thank you

TABLE OF CONTENTS

TABLE OF FIGURES

LIST OF ABBREVIATIONS

ASE	Amplified Spontaneous Emission
CNT	Carbon Nanotube
CW	Continuous Wave
DWFL	Dual-Wavelength Fiber Laser
EDF	Erbium-Doped Fiber
EDFL	Erbium-Doped Fiber Laser
EYDF	Erbium-Ytterbium co-Doped Fiber
EYDFL	Erbium-Ytterbium co-Doped Fiber Laser
FC/PC	Fiber Connector/ Physical Contact
FWM	Four-Wave -Mixing
FWHM	Full Width at Half Maximum
GO	Graphene Oxide
GOSA	Graphene Oxide Saturable Absorber
LD	Laser Diode
MMC	Multimode Combiner
NPR	Nonlinear Polarization Technique

NA	Numerical Aperture
OSA	Optical Spectrum Analyzer
OSC	Oscilloscope
PC	Polarization Controller
PCF	Photonic Crystal Fiber
PDL	Polarization Dependence Loss
PVA	Polyvinyl Alcohol
SA	Saturable Absorber
SESAMs	Semiconductor Saturable Absorber Mirrors
SMF	Single Mode Fiber
SNR	Signal to Noise Ratio
SPM	Self Phase Modulation
SWCNT	Single-Walled Carbon Nanotube
TBF	Tunable Bandpass Filter
WDM	Wavelength Divisional Multiplexer

CHAPTER 1

INTRODUCTION

1.1 Background

A promising alternative to the conventional solid-state laser systems is the fiber laser with some advantages like compact size, high electrical efficiency, superior beam quality and reliability, great output power, lower maintenance, ownership cost, mobility and ruggedness. It was firstly invented by Elias Snitzer (Snitzer, 1961) in 1961 and the first commercial fiber laser devices appeared on the market in the late 1980s. These lasers used single-mode diode pumping, emitted a few tens of milliwatts, and attracted users because of their large gains and the feasibility of single-mode continuous-wave (CW) lasing for many transitions of rare-earth ions not achievable in the more-usual crystal-laser version. They use a specialized optical fiber doped with rare earth elements such as Ytterbium, Erbium and Thulium as the gain medium (Poole et al., 1985). These rare earth elements have many advantages such as simple energy levels, long life time at high level, highly quantum efficiency, and a wide absorption spectrum which finally yield to develop high power fiber laser (Kobtsev et al., 2008) for many applications such as industry, communication, military, and etc.

Most of the developed fiber lasers are based on Erbium-doped fiber (EDF) as the gain medium to operate in 1.5 μm region. Erbium doped fiber lasers (EDFLs) have gained tremendous interest in recent years for optical communication and fiber sensor applications. Many works have also been carried out to develop pulsed EDFL using either active or passive techniques. Active technique is typically performed by inserting optical modulation devices into the cavity (El-Sherif et al., 2003). However, this technique is often relatively complicated due to the presence of the modulators and other bulk devices in the cavity. On the other hand, passive pulse based on saturable

absorbers represents convenient techniques and additional advantages such as simplicity, design of the cavity and compactness (Ahmad et al., 2013; Chang et al., 2012). The efficient generation of short pulses is the strong key qualifying technology in optical communication. Typically, this is recently done by the passive technique based on various saturable absorbers.

Saturable absorbers (SAs) are materials or devices which change their absorbance depends on power of incident light. They absorb the light which has low intensity while the absorbance decreases for the high intensity light. When a saturable absorber is inserted in a laser cavity, amplified spontaneous emission (ASE) noise of a gain medium is shaped to be a pulse train. In every round trip, light pass the saturable absorber as high intensity noise with low loss and low intensity noise with high loss, resulting in high intensity contrast. This finally resulted in the light start to oscillate in pulsed state. Passively mode locked and Q-switched of fiber lasers are generally generated using the SA. These pulse lasers have numerous applications in optical communication, biomedical diagnostics and industrial applications depend on the wavelength, repetition rate, pulse energy and pulse width. In the past research, various SAs have been proposed and demonstrated such as semiconductor saturable absorber mirror (SESAM), graphene oxide and carbon nanotubes (CNTs) (Ahmad et al., 2013; P. Liu et al., 2012; Zhipei Sun et al., 2010) for both passive Q-switching and mode locking applications. The fabrication factors were featured between these SAs in terms of simplicity, compactness, low cost and flexibility in design. However, SESAMs are costly, complex to fabricate, operate in narrow wavelength band and have a low damage threshold and long recovery time for short pulse generation. In contrast, CNT and graphene absorbers are cheaper and simpler to fabricate, operate in wider wavelength band, and have quick recovery times (Z Sun et al., 2009; Tausenev et al., 2008).

This dissertation aims to demonstrate various Q-switched and mode-locked Erbium-doped fiber lasers (EDFLs) using a simple and cheap Graphene-based saturable absorbers. The SA is integrated in the EDFL ring cavity by sandwiching the CNT thin film between two fiber connectors to achieve a stable pulse train with good repetition rate, pulse width and peak power.

In this work, various pulsed fiber lasers operating in both single-wavelength and dual-wavelength modes are proposed and demonstrated using a passive saturable absorber. This dissertation aims to demonstrate various Q-switched and mode-locked fiber lasers operating at 1550 nm region using two different passive techniques; artificial saturable absorber based on nonlinear polarization rotation (NPR) technique and graphene oxide (GO) paper based saturable absorber.

1.2 Problem Statement

Lasers operating in CW or quasi-CW mode have limited optical output power, depending on the maximum available pump power. The laser peak output power can be improved by concentrating the available energy in a single, short optical pulse, or in a periodic sequence of optical pulses as in a Q-switched fiber laser. Q-switching is a technique that enables the generation of an optical pulse at repetition rate in kHz region and pulse width in a range of microseconds to nanoseconds by sudden switching of the cavity loss. Compared to CW fiber lasers, high-peak-power Q-switched fiber lasers are practically useful in numerous applications, such as range finding, remote sensing, industrial processing and medicine (Harun et al., 2012; Kobtsev et al., 2008). Although Q-switching does not produce the ultra-short pulses as in mode-locked lasers, it has several advantages such as inexpensive, easy to implement and efficient in extracting energy stored in upper laser level.

The Q-switched fiber laser can be achieved using either active or passive techniques. Active Q-switching is typically achieved by inserting an acoustic-optic or an electro-optic modulator into the cavity. On the other hand, passive Q-switching by means of saturable absorbers (SAs) is a convenient technique to simplify the cavity design and eliminate the need for external Q-switching electronics. Different kinds of saturable absorbers (SAs), such as the transition metal-doped crystals (Pan et al., 2007) and semiconductor quantum-well structures (J. Huang et al., 2009) have been applied to realize Q-switched fiber lasers especially for operation in 1550 nm region. However, when they are used in the laser cavity, additional alignment devices, such as lens, mirrors or U-bench units, have to be applied. This may increase the insertion loss and the complexity of the laser cavity.

Recently carbon nanotubes and graphene are normally used as the SA for the Q-switched fiber lasers. These SAs are a comparatively simple and cost effective alternative compared to semiconductor SA (SESAM). This is due to their inherent advantages, including good compatibility with optical fibers, low saturation intensity, fast recovery time, and wide operating bandwidth, while the other types of crystal and semiconductor based SAs cannot be used for an all fiber laser structure due to their relatively big volume. In this work, two different low cost approaches are proposed for Q-switching and mode-locking applications. NPR technique is proposed for generating both single-wavelength and dual-wavelength Q-switching pulse trains while GO paper is proposed for both Q-switching and mode-locking applications. Both approaches are new and low cost compared to the existing approaches.

1.3 Research Objective

The main objective of this research is to design and construct an efficient and low cost pulsed fiber lasers operating in 1.5 μm regions using NPR technique and GO paper saturable absorber. This can be achieved by performing the following tasks;

1) To demonstrate a Q-switched fiber laser operating in 1.5 μm regions using a NPR technique.
2) To demonstrate dual-wavelength laser using a NPR technique
3) To demonstrate a single-wavelength and dual wavelength Q-switched laser using a GO paper saturable absorber
4) To demonstrate a mode-locked fiber laser using a GO paper saturable absorber

1.4 Organization of the thesis

This dissertation is organized into five chapters which comprehensively demonstrate the development of pulsed fiber lasers operating in 1.5 μm region using nonlinear polarization rotation (NPR) technique and GO paper SA. Chapter 1 gives a brief description on the recent development of fiber lasers. The motivation and objective of this study are also highlighted. Chapter 2 furnishes a detailed literature on the basic theory of optical fibers, fiber lasers, saturable absorber, Q-switching and mode-locking are described.

Chapter 3 presents a thorough study on Q-switched fiber laser for both single-wavelength and dual-wavelength operations using the NPR technique. Both Q-switched lasers are very attractive because of their compactness, flexibility, and low cost. They have been found in a vast range of applications in recent years including optical imaging, fiber communications, and material processing. The Q-switched fiber lasers are realized by configuring the laser so that the cavity has a sufficiently high loss to prevent mode locking. The gain medium is a double-clad Erbium-Ytterbium co-Doped Fiber (EYDF),

which is pumped by a multi-mode 980 nm pump. In this approach, an isolator is used in conjunction with a highly nonlinear EYDF in a ring cavity to induce intensity dependent loss and initiate Q-switching pulse.

Chapter 4 aims to develop Q-switched and mode-locked fiber laser operating at 1550 nm region using a commercially available non conductive graphene oxide paper as a saturable absorber. The SA was fabricated by sandwiching a small piece of a commercial GO paper between two FC fiber connectors. The easy fabrication of graphene oxide paper will promote its potential in Q-switching and mode-locking applications. Finally, Chapter 5 summarizes the findings for this MPhil work.

CHAPTER 2

LITERATURE REVIEW

2.1 Introduction

The development of the LASER (Light Amplification by Stimulated Emission of Radiation) was the first important step in the establishment of the fiber optics industry. Fiber lasers are one type of laser that has gone through intense development in the last two decades.They are compact, reliable and environmentally stable compared to their bulk counterparts and are ideally suited in many applications such as material processing, telecommunications, spectroscopy and medicine. Despite the progress already made by fiber lasers, there is still much room for the development of new lasers intended for specific applications. The objective of this thesis is to develop a low cost pulsed fiber lasers operating at 1.5 μm spectral region using an erbium-ytterbium co-doped or Erbium-doped fibers as the gain medium and passive saturable absorber. There are a number of interesting principles that come into play in the operation of the Q-switched and model-locked Erbium-doped fiber laser (EDFL). This chapter briefly introduces the main principles relevant to understanding the operation of such lasers.

2.2 Optical fibers

An optical fiber is a coaxial cylindrical dielectric wave-guide designed to transmit EM waves at optical frequencies. Optical fibers were first proposed and produced by K.C. Kao and G.A. Hockham in 1966 (Kao et al., 1966). Since this development, refinements in fiber design and fabrication processes have led to the production of fibers with low dispersion and losses (0.2 dB/km), and optical fibers now hold a prominent place as the backbone of communication systems. The material of

choice for most telecommunications-grade optical fibers is fused silica glass. A glass becomes a viscous fluid above the glass transition temperature with its viscosity decreasing continuously as the temperature is further increased (Kao et al., 1966). This property makes the silica glasses ideal for drawing into thin fibers of arbitrary and controllable thickness when heated to temperatures at which they become soft and ductile. The resulting fibers are extremely durable, with tensile strengths as high as steel wires of the same diameter, and are resistant to degradation by most chemicals at ambient temperatures (Kapron et al., 1970). Most importantly for communication, pure silica is highly transparent at optical frequencies, allowing transmission distances of hundreds of kilometers at 1550 nm wavelength band region (Miya et al., 1979).

An optical fiber, in its simplest form as shown in Figure 2.1(a), consists of a cylindrical core (radius R_{core}: a few to several tens of micrometers) that is surrounded by a cladding (radius R_{clad}: a few tens to several hundreds of micrometers). The refractive index of the core (n_{core}) is slightly higher than that of the cladding (n_{clad}), which satisfies the condition for total internal reflection (TIR) at the core-cladding interface (Figure 2.1(b)). Therefore, ideally, light can be confined inside the core without any propagation loss. For a step-index fiber, the index distribution along its radial direction is:

$$n(r) = \begin{cases} n_{core}(\ 0 < r < r_{core}\ ) \\ n_{clad}(\ R_{core} < r < r_{clad}\ ) \end{cases} \tag{2.1}$$

Where r is the radial coordinate. Light is confined within the core of a step index fiber by means of total internal reflection at the core-cladding interface. Light rays incident on the fiber end face within a certain angle known as the acceptance angle will couple into the fiber (Figure 2.2). The maximum angle of incidence "θ_{max}" for coupling to the fiber is related to the core and cladding refractive using Snell's Law.

$$n \sin \theta_{0,\max} = (n_1^2 - n_2^2)^{1/2} \tag{2.2}$$

The quantity $n \sin \theta_{0,\max}$ quantifies the light accepting capability of a fiber and is known as the numerical aperture (NA).

The NA of the fiber, which represents the maximal acceptance angle within which the TIR condition can be satisfied, may be expressed by:

$$NA = \sqrt{n_{core}^2 - n_{clad}^2} \approx n_{core}\sqrt{2\Delta} \tag{2.3}$$

where $\Delta = (n_{core}-n_{clad})/n_{core}$ and $n_{core} \approx n_{clad}$ is assumed for weakly guiding fibers.

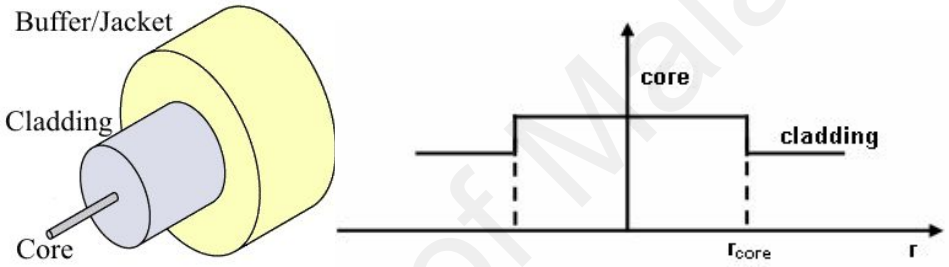

Figure 2.1: (a) Schematic diagram of a standard step-index optical fiber and (b) Its refractive index profile

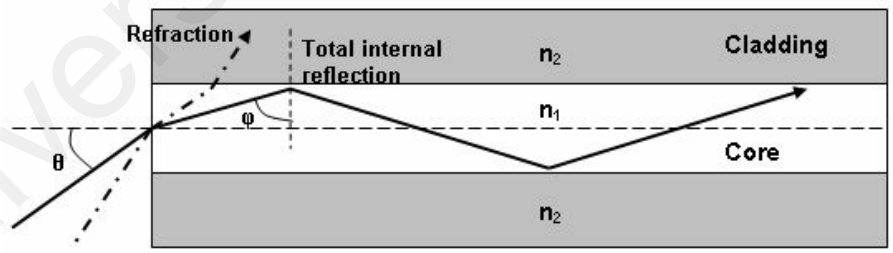

Figure 2.2: Confinement of light within the fiber core by total internal reflection.

2.3 Fiber laser fundamental

The generation of light in an Erbium-doped fiber (EDF) can be described using a three level lasing model, since the Erbium ions exist primarily in one of three energy

levels (Figure 2.3). The energy levels are labeled with respect to the ground level E_1. E_2 is the metastable level, where the term metastable implies that the lifetimes for transitions from this state to the ground state are very long compared with the lifetimes of the higher energy states. E3 is the pump level; the pump band is fairly narrow, and so the pump wavelength must be exact to within a few nanometers.

Typically, a pump laser emitting 980 nm photons is used to excite ions from the ground state to the pump level. These excited ions decay (relax) very quickly (around 1 μs) from the pump band to the metastable band. During this decay. The excess energy is released as phonons (or equivalently thermal energy) in the fiber. Within the metastable band, the electrons of the excited ions tend to populate the lower end of the band due to thermodynamic considerations. Some of the ions sitting at the metastable level can decay back to the ground state in the absence of an external influence. This process is known as spontaneous emissions and adds noise to the system.

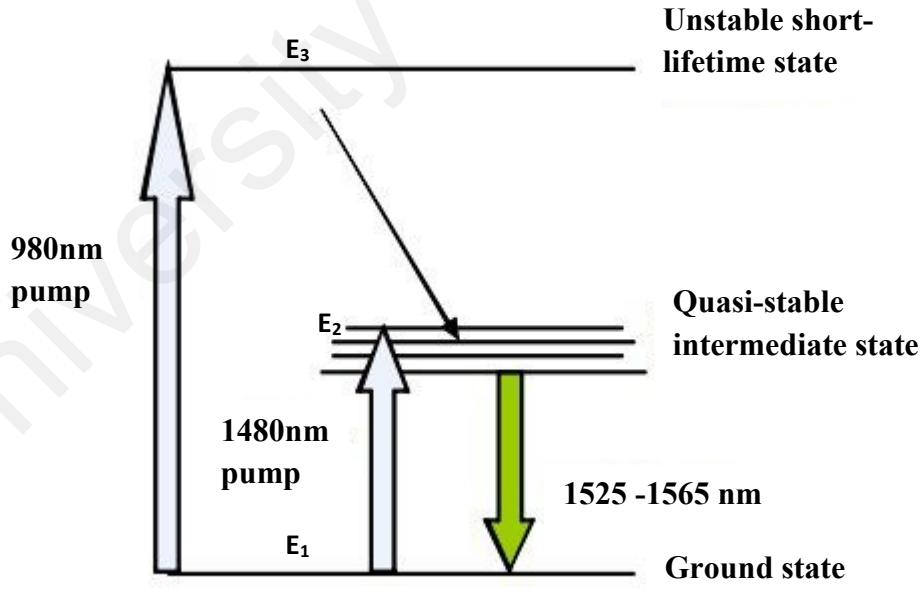

Figure 2.3: Simplified energy-level diagram of Erbium ions

When a signal photon with energy corresponding to the band-gap energy between the ground state and the metastable state passes through the system, two other types of

transitions take place. First, it is possible for photons to be absorbed by ions in ground state, which raises these ions to the metastable level (process 4).This is known as stimulated absorption.Second, a photon can trigger an excited ion drop to the ground state, thereby emitting a new photon of the same energy, wavelength and polarization as the incoming signal photon (process 5). This process is known as stimulated emmision and it is the mechanism providing amplification in an EDFL. The widths of the metastable and ground state level allow high levels of stimulated emission to occur in the 1530 to 1560 nm range.

Amplification of light in a section of pumped EDF is achieved by feeding the output back into the input of the EDFL to form an optical resonant cavity. Allowing some of the light within the resonator to escape as usable light result in a potential source of EDF laser light. There are two basic resonator designs for fiber laser, the traveling wave ring resonator and the standing wave Fabry-Parot resonator.This section will focus on the traveling wave ring resonator depicted in Figure 2.4. It should be noted that there is no external input signal (at the lasing wavelength) applied to the cavity, although external pump light is injected.The lasing signal is essentially by a small amount of spontaneous emission created upon initial pumping.If the gain and phase condition are met, lasing within the cavity will occur, producing continuous light.

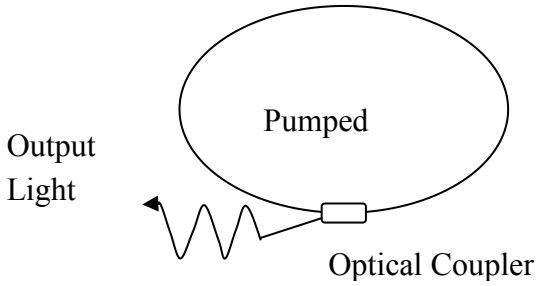

Figure. 2.4: Traveling wave ring resonator

2.3.1 Gain condition for laser operation

For a traveling wave ring resonator, the round trip gain must be equal to or greater than the round trip loses. The minimum gain coefficient value γ_{th} required for lasing is given by;

$$\gamma_{th} = L - \frac{\ln R}{l} \tag{2.3}$$

where: R= effective fractional power reflectivity of the coupler or ($R=1-C$), C = Output power coupling ratio, L = the total lumped fractional intensity loss per round trip, l =the total round trip distance (one round-trip equal the total ring circumference)

2.3.2 Phase Condition for lasing

The phase requirement for laser operation is that an integer number of resonating wavelengths must fit within one round trip of the laser's resonant cavity. For an EDF ring laser, since the length of the cavity is very long relative to the resonant wavelength, there are many wavelengths, referred to as longitudinal modes, which satisfy the phase condition.

For a multi-longitudinal mode operating ring resonator, the expected frequency spacing df between modes is given by:

$$df = \frac{c}{nl} \tag{2.4}$$

Where c is the speed of light in vacuum, n is the optical refractive index and l is the cavity length (ring circumference). The typical amplification range (gain bandwidth) for EDF span over 30nm, from 1530 nm to 1560 nm as depicted in Figure 2.5, imllying that many longitudinal operating modes can possibly satisfy the gain and phase condition for lasing. Hence EDF lasers have the potential to be highly multi-mode lasers. The light generated within each mode is coherent (intra-modally coherent) but it is incoherence

between different modes (intermodally incoherent). Each of these modes oscillate independently, with no fixed relationship, in essence like a set of independent lasers all emitting light at slightly different frequencies. The individual phase of the light waves in each mode is not fixed and may vary randomly.

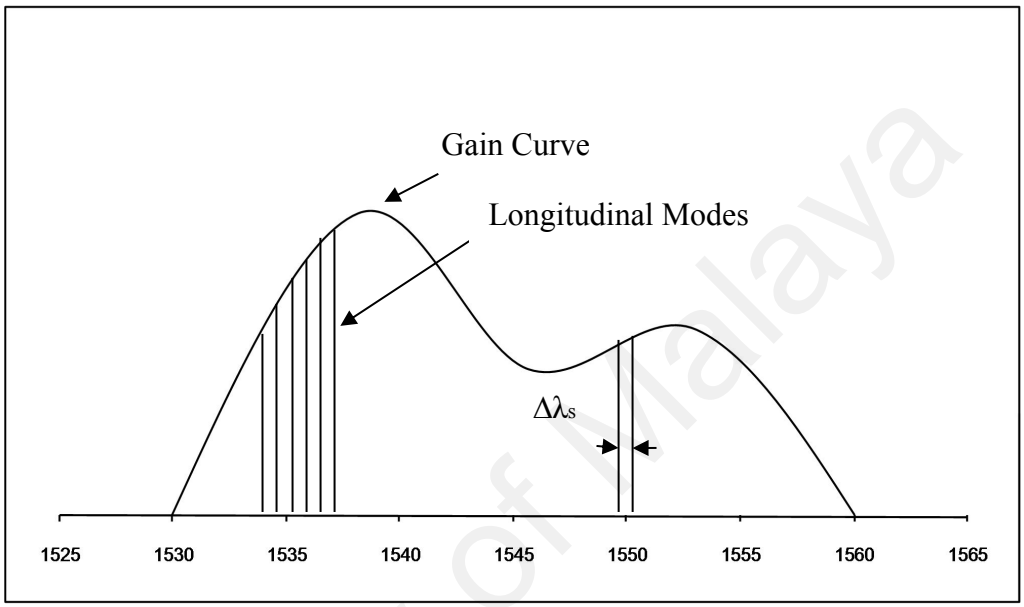

Figure 2.5: Gain curve depicting the many longitudinal modes that could satisfy the gain and phase requirements for lasing. Δλs is the wavelength spacing between modes

For a continuous wave laser, this multi-modal behavior is undesirable and various measures (Park et al., 1991) can be taken to ensure that the laser operate at only one of the many possible longitudial modes. Mode locked lasers take advantage of the large gain bandwidth and this multi-modal behavior to produce ultra short, high-energy pulses. If instead of oscillating independently, each mode operates with a fixed phase between it and the others modes, the modes will constructively interfere with bone another, producing intense bursts or pulses of light. Such a laser is said to be mode-locked.

Optical fibers have played an essential role in the development of modern telecommunication systems. The great era of optical fiber communications would never

have been possible without the appearance of low-loss optical fibers. The propagation loss of early fibers had been high (～1000 dB/km) at the telecom wavelength of 1.5 μm (Kapany, 1967), but it was drastically reduced to 20 dB/km in early 70s (Kapron et al., 1970) and was soon reduced to 0.2 dB/km (Miya et al., 1979). Fibers for long-distance optical signal transmission were ready and long haul optical networks became practical, therefore started the revolution in the field of telecommunications. Optical fibers were initially designed solely for purpose of light transmission, however their unique light guiding property quickly attracted them to other applications. One important application is to fabricate compact light amplification and lasing devices by doping the fiber cores with rare-earth ions. A compact low-threshold high-gain optical amplifiers and lasers were realized via a process of stimulated emission by using an active fiber as the gain medium. Optical fiber used as laser gain medium was first demonstrated in 1964 (Koester et al., 1964), shortly after the first laser appeared (Maiman, 1960), and the first fiber lasers were realized in 70s in both pulsed (J Stone et al., 1973) and continuous-wave (CW) (Joshua Stone et al., 1974) forms.

The most common laser cavity used by fiber laser is the Fabry-Perot resonator, as shown in Figure 2.6. It is typically constructed by placing a piece of active fiber butted against two planar dielectric mirrors, one serves as the input coupler and the other as the output coupler. Both ends of the fiber are either perpendicularly cleaved or polished flat. Dielectric coatings can also be directly deposited on the fiber facets to replace the bulk mirrors and serve as the input and output couplers. Pump power is directly focused into the fiber by pump launching optics through the input coupler, which is transparent to the pump light and highly reflective to the signal light. The signal leaves the laser cavity through the output coupler, which can maximize the laser efficiency from dual aspects: its high reflectivity at the pump wavelength can send any

unabsorbed pump light back into the cavity and its reflectivity at the signal wavelength can be optimized to maximize the output power.

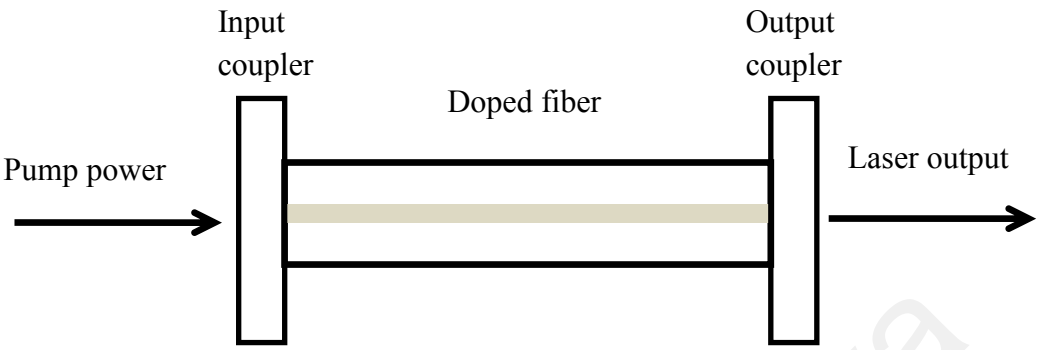

Figure 2.6: Schematic drawing of a fiber laser configured with Fabry-Perot resonator.

Rare-earth ions, e.g., neodymium (Nd^{3+}), ytterbium (Yb^{3+}), erbium (Er^{3+}), thulium(Tm^{3+}), holmium (Ho^{3+}), samarium (Sm^{3+}), and praseodymium (Pr^{3+}) have long been used for optical applications at the near infrared spectral range. Nd^{3+} is the first rare-earth ion introduced into fibers that demonstrated high gain (Koester et al., 1964) and laser operation (Joshua Stone et al., 1974) at near infrared; Yb^{3+}-doped fibers emit a broad spectral range from 970 to 1200 nm (Etzel et al., 1962; Pask et al., 1995; Suni et al., 1990); Er^{3+}-doped fibers emit at the important telecom wavelength of 1.5 μm (Mears et al., 1986; Reekie et al., 1986); while Tm^{3+}- and Ho^{3+}-doped fibers operate at the relative long wavelength around 2 μm (Hanna et al., 1988; Hanna et al., 1989). Figure 2.7 illustrates the wavelength ranges demonstrated in rare-earth doped silica fiber lasers.

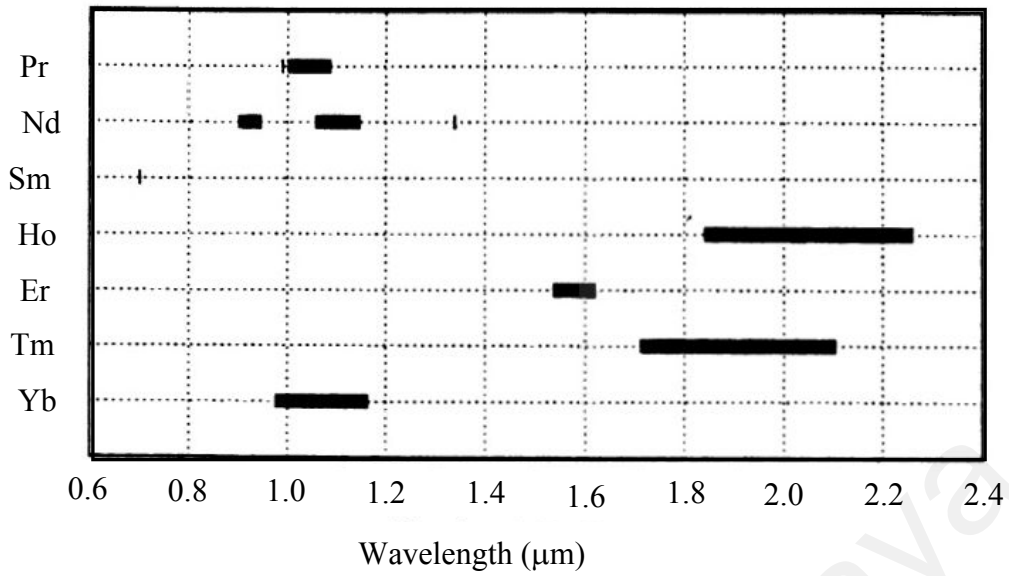

Figure 2.7: Wavelengths demonstrated in CW rare-earth-doped silica fiber lasers (Digonnet, 2001)

Since the introduction of fiber lasers in 60s and 70s, drastic improvement in laser performance and efficiency was achieved in 1980s with the realization of low-loss rare-earth-doped silica fibers (Mears et al., 1985; Poole et al., 1985), the application of semiconductor laser diodes as pump sources, and novel designs of fibers and pumping schemes. The early fiber lasers and amplifiers had only one effective wave-guiding component: the core. Since both the signal and pump light are guided in the core, for the fiber lasers to achieve efficient and robust laser operation, the pump light emitted from laser diodes needs to be coupled into the small core area with high efficiency and stability. This requires the laser diodes to be single-mode and have high brightness. However, high-power single-mode laser diodes remain to be a technique challenge up to date and the output powers from the core-pumped fiber lasers are still limited to ~1 W due to the pump power availability.

To break this stringent pump source requirement and take advantage of the available high-power multi-mode laser diodes of relative low brightness, cladding-pumped fiber devices were introduced in late 80s (Snitzer et al., 1988). Double-clad fibers are designed for the cladding-pumping scheme, as shown in Figure 2.8, a second

(outer) cladding with lower index than that of the first (inner) cladding is added. The pump light is injected into the inner cladding and is confined there, because the TIR condition is satisfied at the inner-outer cladding interface. At the same time, since only the core is doped and the signal light is generated and confined inside the core, the signal will still have a high brightness regardless of the properties of the pump light.

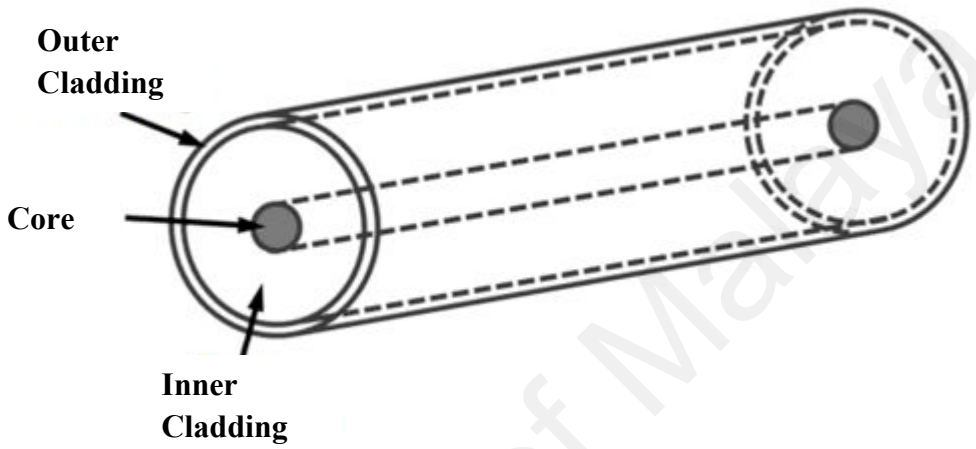

Figure 2.8: Schematic diagram of a double-clad fiber

Another major advantage of the cladding-pumping scheme is that these fiber laser shave high thermal tolerance for high-power CW laser operation. Though the pump power fills out the inner cladding during its propagation along the fiber, only the core region absorbs the pump light. The pump absorption coefficient of the fiber is thus proportional to the ratio of core area over the inner cladding area, if the pump power is evenly distributed across the cross-section of the inner cladding. Therefore, one can always lower the core doping level and increase the inner cladding size to effectively reduce the pump absorption coefficient, at the same time, elongate the fiber length to ensure sufficient pump absorption. Another thermal concern is that as laser diode arrays of very high CW power are available, the output power of the fiber laser can be limited by the breakdown of the active core region, due to the high optical power density at the single-mode core centre. To reduce the intensity at the core centre, large and slightly

multi-mode cores can be used instead of the small single-mode cores. Though large cores may allow a few transverse modes, careful designs and special techniques, such as bending, can be used to strip out the high order modes so that the large cores can still be under fundamental mode operation. Large core size will also help overcome yet another power scaling limitation factor: the nonlinear effects such as stimulated Raman and Brillouin scatterings. Since the threshold powers of these nonlinear effects are proportional to the effective modal area, large cores will enhance the threshold powers and postpone the output power rollover caused by nonlinear effects to a later stage in power scaling. The high level of output powers and reduced risk of thermal damages make cladding pumped rare-earth-doped near infrared fiber lasers excellent candidates to replace conventional bulk solid-state lasers for many applications, such as remote sensing, LIDAR, medicine, material processing, and industrial machining.

2.4 Working principles of fiber lasers

Gain medium, pump and optical cavity are three main elements of laser. These elements work together to produce the laser output. Gain medium can be a solid (crystal, glasses), liquid (dyes or organic solvents), gas (helium, CO2) or semiconductor. Pump can be optical, electrical, chemical, or thermal. Optical cavity is containing the lasing medium, with either linear or ring configuration. A fiber laser is basically a laser oscillator in which a section of rare earth doped fiber rare-earth elements such as erbium, ytterbium, neodymium, dysprosium, praseodymium, and thulium serves as the gain medium. The operation of a laser requires photons created in the laser cavity. This is achieved by an external pump source which provides energy that can be coupled into the laser medium that can excite the atoms and create the required population inversion. According to Einstein in his famous paper of 1917 when the population inversion exists between upper and lower levels among atomic systems, it is possible to realize

amplified stimulated emission (ASE) and the stimulated emission has the same frequency and phase as the incident radiations. The Ytterbium-doped fiber lasers for example use 980 nm pumping o generate laser at 1050 nm region.

Figure 2.9 illustrates absorption, spontaneous emission and stimulated emission processes in gain medium of fiber lasers. When an electromagnetic wave with frequency ω traveling along the *x*-axis and polarized along the *z*-axis is incident on an atom in the ground state, the oscillating electric field of the EM wave can induce an electronic transition to an excited state, with the atom absorbing energy $h\omega_o=E_b-E_a$ (Figure 2.9(a)). If another photon of the same frequency interacts with the same atom while it is still in the excited state, it can induce a transition back to the ground state (Figure 2.9 (c)).This transition occurs with the same probability as the excitation from the ground state and leads to the emission of two photons of energy $h\omega_o$ with the same phase and polarization. The above phenomenon is known as stimulated emission. In order for stimulated emission to lead over absorption, population inversion is necessary, which is achieved by pumping the amplifying medium. Pumping is carried out by transferring energy to the amplifying medium in order to induce transitions to the excited state. Population inversion is achieved when a greater number of atoms live in the excited state than the ground state. Another important element for laser oscillation is a resonant cavity to direct the signal radiation through the amplifying medium repeatedly, allowing a high intensity wave to build up within the cavity (Figure 2.4).

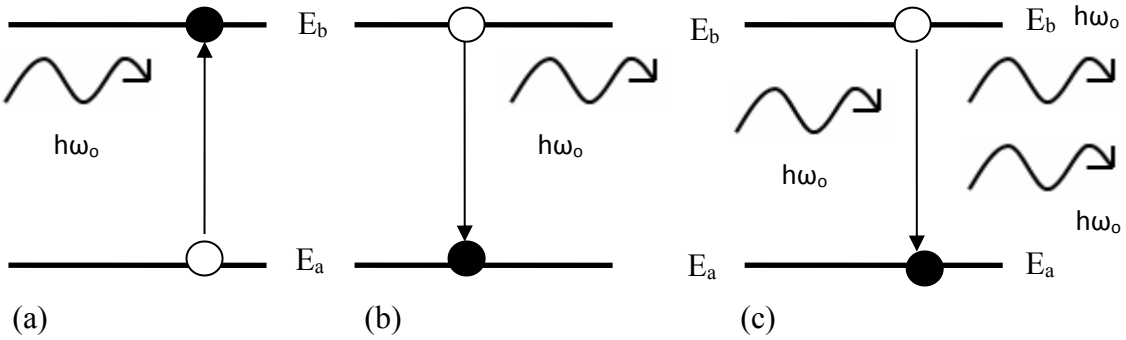

Figure 2.9: a) Absorption of a photon with energy $h\omega_o$ inducing a transition from the ground state *"a"* to the excited state *"b"*. b) Spontaneous emission of a photon resulting in a transition from the excited state to the ground state. c) Stimulated emission.

2.5 Ytterbium fiber laser

Ytterbium (Yb) is a chemical element belonging to the group of rare earth metals. In laser technology, it has acquired a prominent role in the form of the trivalent ion Yb^{3+}, which is used as a laser-active dopant in optical fiber for both generations.Ytterbium-doped fibers (YDFs) have a number of interesting properties. They have a very simple electronic level structure, with only one excited state manifold ($^2F_{5/2}$) within reach from the ground-state manifold ($^2F_{7/2}$) with near-infrared or visible photons. Pumping and amplification region of the YDF is shown in Figure 2.10, which involve transitions between different sub levels of the ground-state and excited-state manifolds.As shown in the figure, the Yb^{3+} ion possesses a number of emission transitions within the 974 – 1068 nm wavelength range. The homogeneous and in homogeneous broadening of these transitions within a glass host leads to a wide and continuous emission spectrum in the 1 micron band.

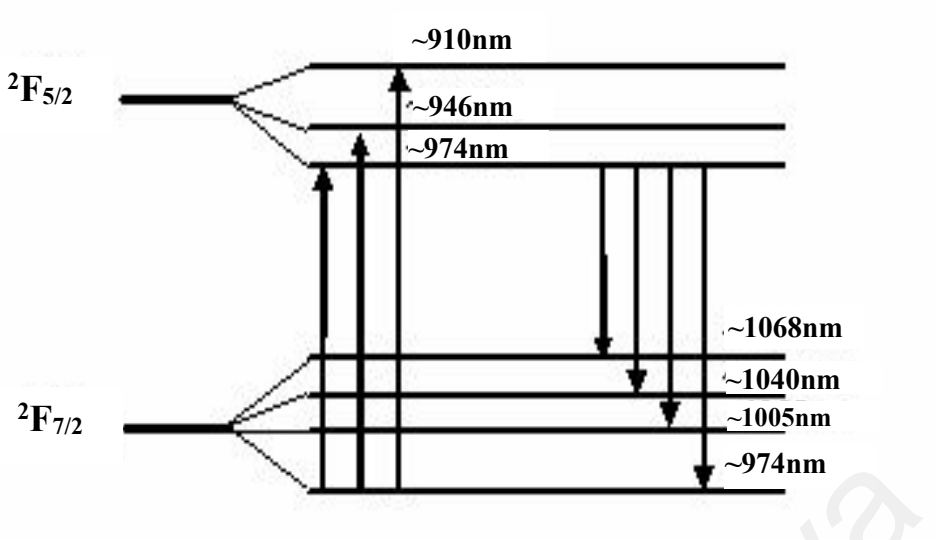

Figure 2.10: Energy levels diagram of a YDF, and the usual pump and laser transitions.

The YDF laser have a few advantages compared to other types of lasers such as Nd doped laser and Erbium-doped fiber lasers. The quantum defect of Yb ion is always small, potentially allowing for very high power efficiencies of lasers and reducing thermal effects in high-power lasers. It also has a simple electronic structure, which prevents excited-state absorption and also a variety of detrimental quenching processes.The gain bandwidth of the laser transitions is typically fairly large, compared with, neodymium-doped lasers. This allows for wide wavelength tuning ranges or for generating ultrashort pulses in mode-locked lasers in 1 micron wavelength region. The upper-state lifetimes are relatively long (typically of the order of 1–2 ms), which is beneficial for Q switching.

Ytterbium doping is also often used together with erbium doping, where ytterbium ions typically absorb the pump radiation and transfer the excitation energy to erbium ions. Even though the erbium ions could directly absorb radiation e.g. at 980 nm, ytterbium co-doping can be useful because of the higher ytterbium absorption cross sections and the higher possible ytterbium doping density in typical laser glasses, so that a much shorter pump absorption length and a higher gain can be achieved. The

distribution of energy levels of Er^{3+} and Yb^{3+} ions in the host determines the basics pectroscopic properties of the doped material as well as its potential applications. Both Er and Yb belong to the group of lanthanides that cover atomic numbers from 57 to 71.Er atom (atomic number 68) has an electronic structure of $(Xe)4f^{12}6s^2$, where (Xe)represents the electronic structure of xenon (atomic number 54), and Yb atom (atomic number 70) has an structure of $(Xe)4f^{14}6s^2$. When Er and Yb atoms are ionized, they first lose two loosely bounded $6s^2$ electrons and then one 4f electron. So Er^{3+} and Yb^{3+} ion shave electronic structures of $(Xe)4f^{11}$ and $(Xe)4f^{13}$, respectively. Since (Xe) is a very stable structure, the energy levels of these trivalent ions are dominated by the properties of the 4f electron shells. The energy levels of Er^{3+} and Yb^{3+} in glasses are shown in Figure 2.11. Note that each energy level in Figure 2.11 is not a single line, but a manifold of broadened line width that is decided by both the homogeneous and in-homogeneous broadening mechanisms in solid hosts (Becker et al., 1999).

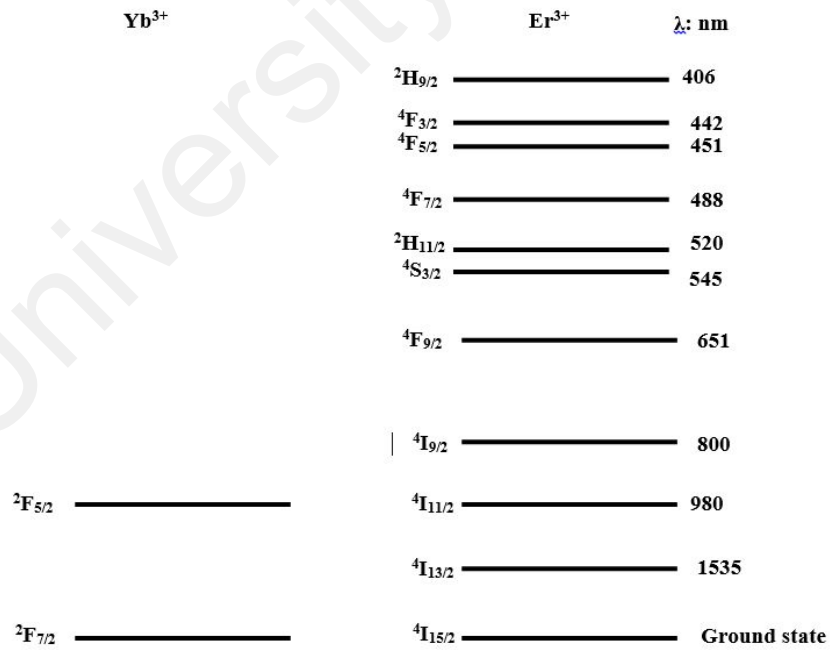

Figure 2.11: Distributions of energy levels of $Er^{3+}$and Yb^{3+}ions in glass.

The main laser transition of interest in Er^{3+} is the $^4I_{13/2}$ to $^4I_{15/2}$ transition centre around 1.5 μm. This is essentially a three level laser system: $^4I_{15/2}$ ground state serves as the lower lasing level and $^4I_{13/2}$ is the upper lasing level that is filled by ions from $^4I_{11/2}$ level through fast decay. The key to the success of this laser transition is that $^4I_{13/2}$ level is separated by a large energy gap from the $^4I_{15/2}$ ground state, so that its lifetime is long and mostly radiative. The average lifetime is about 10 ms, depending on the host material and Er^{3+} concentration, and this long lifetime allows population inversion to be induced by a relatively weak pump power density. Possible pumping wavelength for the 1.5 μm laser transition can be at 1480 nm, 980 nm, 800 nm, and even in the visible such as 651 nm, 545 nm and 520 nm. Pumping at 980 nm is a very appealing choice: it is free of excited state absorption and high-power 980 nm laser diodes are commercially available.Yb^{3+} has long been known as an excellent co-dopant for Er^{3+}-doped fibers to improve the 980 nm pump absorption (Snitzer et al., 1965). The criterion to select the proper co-dopant is obvious: it should absorb the pump light much stronger than the laser ion and the absorbed energy can be efficiently transferred to the latter. Figure 2.12shows how the 1550 nm laser is achieved in principle by Erbium Ytterbium co-doped fiber (EYDF) via 980 nm pumping. As seen in the figure, Yb^{3+} ions absorb pump photons and are excited from $^2F_{7/2}$ ground state to $^2F_{5/2}$ state, then they efficiently transfer the absorbed energy to excite Er^{3+} ions to $^4I_{11/2}$ level, and Er^{3+} ions eventually arrive at $^4I_{13/2}$ level by fast non-radiative decay. Ytterbium co-doping can also be used for Thulium-doped fiber lasers operating at 2 micron region.

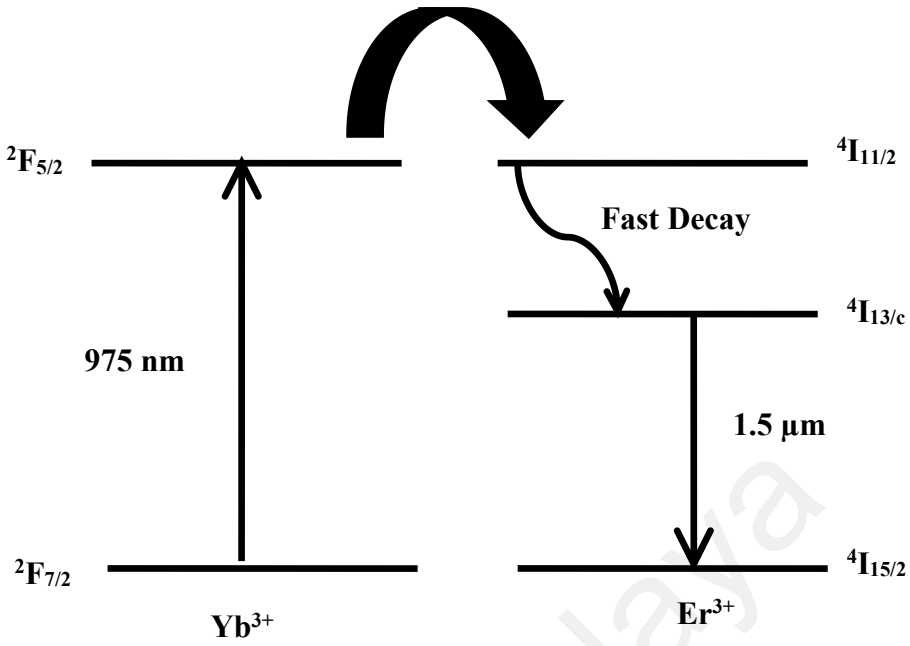

Figure 2.12: Working principle of the EYDF laser operating at 1550 nm using a 980 nm pumping.

2.6 Q-switched fiber laser

Owing to their inherent technological advantages, pulse fiber lasers are increasingly becoming the light source for a wide range of industrial and scientific applications. Pulse fiber lasers can be generated based on two techniques; Q-switching and mode-locking. One of the main objective of this thesis is to generate Q-switching pulse train in 1.0, 1.5 and 2 µm micron region using a YDF, EYDF and TYDF, respectively. These Q-switched laser shave many possible applications especially in laser light detection and ranging (LIDAR), medicine and remote sensing.

In general, Q-switching is a technique used to generate energetic pulses, with duration typically in the range of nanoseconds to microseconds, by modulating intra-cavity losses of a laser. When the losses of a resonator is varied, the resonator Q–factor is also varied, resulting in a so called Q-switched operation. The intra-cavity loss-modulation can be performed actively using, for instance, modulators or passively saturable absorbers. Basically, the laser pumping builds up a large inversion producing

large gain while the resonator losses are sustained at high levels. Suddenly, the resonator losses are minimized, therefore result in the energy stored in the cavity is released in the form of an intense pulse. Typically, Q-switched lasers are employed in applications that require high pulse energies and peak powers with reasonably high average powers and short pulses.

Compared to the active technique, passive Q-switched fiber lasers are more compact and simple. They can be realized by inserting a nonlinear optical device called a saturable absorber (SA) into the laser cavity. In principle, most light-absorbing materials can be used as SAs in their resonant absorption wavelength range. Indeed, over the past couple of decades, a large range of SA materials have been demonstrated, including dyes, color filter glasses, dye- or ion-doped crystals and glasses, metal nano particles and semiconductors. Unfortunately, all these SAs have their own drawbacks, and are thus unable to satisfy the key SA requirements for pulse fiber lasers, such as fast response time, strong non linearity, broad bandwidth, low loss, high power handling, low cost, and simplicity of fabrication and integration into various optical fiber systems.

Current commercial pulse lasers generally use semiconductor SA mirrors (SESAMs). The excellent performance of SESAMs is mainly credited to the well-developed semiconductor technologies for electronics (for example, band gap and defect engineering and growth techniques). This allows good control over the SA parameters, and thus SESAMs currently are the primary SAs employed for Q-switching. However, the fabrication of SESAMs generally involves complex, highly specialized equipment to being expensive and either post-growth ion implantation or low-temperature growth to reduce the device response time.

Recently, carbon nanotubes (CNTs) and graphene have gained tremendous attention due to their excellent electrical and optical properties, which enable them to be used for various high performance electronic and photonic devices. In particular, their

unique nonlinear optical properties make them ideal to be implemented in a wide range of photonic devices, such as saturable absorbers, ultra-fast optical switches, and wavelength converters. SAs based on single-walled carbon nanotubes (CNTs) were first developed in 2003, and have subsequently been rapidly adopted by several groups because they are relatively simple and inexpensive to fabricate. These SAs are particularly advantageous for fiber lasers because they can be easily integrated into various fiber configurations while preserving an alignment-free, all-fiber format. For example, CNTs or their polymer composites can be sandwiched between two fiber connectors as shown in Figure 2.13.

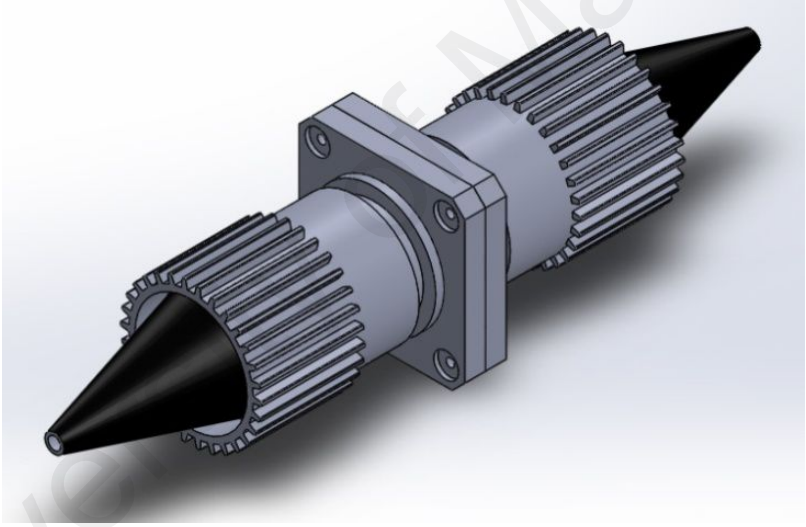

Figure 2.13: Sandwiched device for integrating CNT and graphene film based SA into a fiber laser cavity.

2.7 Important Laser Parameters

Laser threshold and output power

Laser threshold is defined as the minimum amount of pump power or energy to starts the lasing action in which the gain coefficient is large enough to overcome the losses in the cavity. The output is considered to be a laser when the pump power is sufficiently high such that population inversion is achieved and therefore, the energy of the system has reached the lasing threshold. According to Figure 2.4, fiber gain will oscillate in the cavity length, L between two reflecting mirror, which are almost fully transmitting and partially transmitting, $R_1$and R_2. Thus, the fraction of light remaining after a full round trip time through the laser denoted by:

$$e^{-2\gamma} = R_1 R_2 \tag{2.6}$$

where γ is the measured loss in a single passage and positive, therefore:

$$\gamma = -\frac{1}{2}\ln\left(\frac{1}{R_1 R_2}\right) \tag{2.7}$$

the intensity of the radiation increased as the laser oscillates in the cavity due to the continuous population inversion by a factor of $e^{\beta L}$ where β is amplification coefficient. β is given by $\beta(\nu)=\kappa(\nu_0)\Delta N$, where $k(\nu_0)$ is the absorption coefficient at maximum wavenumber, ν and ΔN is the population inversion. Comparing the increased intensity of the radiation in a passage and the fraction of light remains in the cavity, the threshold of laser oscillation is attained when the peak value β of the amplification satisfies the condition below (Reisfeld et al., 1977)

$$\beta L > \gamma \tag{2.8}$$

The threshold power usually depends on the gain per unit pump power, the round trip cavity losses, and the how strong the pump, signal and dopant are confined (Armitage, 1988). Thus a lower threshold can be achieve by reducing the core size, and increasing the NA of the fiber (Digonnet et al., 1990).

Slope efficiency

The slope efficiency is one of the important parameters in characterizing a laser. The efficiency of the laser is given by the output power of the laser, P_{out}, for a given peak power pumping, P_{in}. For a system in a low loss cavity and assuming the absent of ESA pumping, the output power, P_{out} is given by (Digonnet, 2002)

$$p_{out} = \frac{T_1}{\delta_0}\frac{h\nu_S}{h\nu_p}\left(P_{abs} - P_{th}\right) \tag{2.9}$$

Where $h\nu_s$ and $h\nu_p$ is the signal photon energy and pump photon energy respectively. T_1 is the power transmission of the output coupler, δ_0 is the round-trip loss, P_{ab} is the total pump power absorbed by the dopant and P_{th} is the threshold power. The Eq. (2.7) states that the output power grows linearly with absorbed pump power. Thus, the slope efficiency, defined as the output power divided by the power absorbed in excess of threshold P_{abs}-P_{th} is (Digonnet, 2002)

$$\eta_S = \frac{T_1}{\delta_0}\frac{h\nu_S}{h\nu_p} \tag{2.10}$$

The slope efficiency is proportional to the ratio λ_p/λ_s of the pump and signal wavelengths. The efficiency depends on the slope of the graph. This is due to the active pump photon compared to the signal photon in order to excite ions to the higher level, and the energy difference between them is wasted usually in terms of phonons.

Chapter 3

Q-switched Fiber Laser Based on Nonlinear Polarisation Rotation Technique

3.1 Introduction

Lasers operating in CW or quasi-CW regime have limited optical output power, depending on the maximum available pump power. By concentrating the available energy on a single short optical pulse, or in a periodic sequence of optical pulses, higher peak power is attainable. Q-switching is a technique that enables the generation of short optical pulses by means of repeated switching of the cavity loss (Harun et al., 2012; Kobtsev et al., 2008; Wang et al., 2007). Compared to CW fiber lasers, high-peak-power Q-switched fiber lasers are practically useful in numerous applications, such as range finding, fiber sensing, industrial processing, communication and biomedical(Harun et al., 2012; Kobtsev et al., 2008). Traditionally, active Q-switching methods using optical modulation devices, such as acousto-optic modulators(Wang et al., 2007) and electro-optic modulators (Fan et al., 2004) are the most widely adopted schemes in Q-switched lasers. Due to the presence of the modulators and other bulk devices in the cavity, the configurations of the widely-used, actively Q-switched solid-state lasers are often relatively complicated (Lin et al., 2007). With the increasing popularity and performance improvement of fiber lasers, Q-switched Erbium-doped-fiber (EDF) lasers have attracted more and more attention, which could have advantages in their size, weight and cost (Chang et al., 2011; H.-Y. Wang et al., 2012). On the other hand, in contrast to the actively Q-switching schemes, the passively Q-switching techniques could have additional advantages such as simplicity and compactness.

Recently, nonlinear polarization rotation (NPR) technique has been widely used to provide an artificial SA effect in a mode-locked fiber ring laser (Hamzah et al., 2013). Moreover, the NPR technique provides an intrinsic feature of spectral filter induced by the combination of polarizer and intra-cavity birefringence, which can be used to achieve the multi-wavelength and wavelength-tunable operation in the fiber ring laser. For instance, Luo et. al. employed the NPR induced spectral filtering effect to develop wavelength tunable passively mode-locked fiber laser (Luo et al., 2010). However there is still a lack of research work on the use of NPR technique in realizing Q-switched pulses.

In this chapter, Q-switched fiber lasers operating in single-wavelength and dual-wavelength operations are proposed and demonstrated based on the NPR technique by configuring the laser so that results in sufficiently high cavity loss to prevent mode locking. The gain medium is a double-clad Erbium-Ytterbium co-Doped Fiber (EYDF), which is pumped by a multi-mode 980 nm pump. In this approach, an isolator is used in conjunction with a highly nonlinear EYDF in a ring cavity to induce intensity dependent loss and initiate Q-switching pulse.

3.2 Q-switched fiber laser operating in 1.5 μm

In this section, Q-switched EYDF laser (EYDFL) is proposed and demonstrated using an NPR technique. Figure 3.1 shows the proposed configuration, which consists of a 5 m long double-clad EYDF, a multi-mode combiner (MMC), an isolator, a polarization controller (PC) and 95/5 output coupler in a ring configuration. The EYDF used has a core, inner and outer cladding diameters of 5 μm, 105 μm and 125 μm respectively. Inset of Figure 3.1 shows the cross-section image of the EYDF, which has a multi lobed pump guide structure. The core has a numerical aperture 0.21 whereas the

pump guide (inner cladding) has the NA of 0.25. The multi-lobed inner cladding shapes are helpful in ensuring all the rays corresponding to pump power propagating in the inner cladding cross the core, this leads to increase the pump conversion efficiencies. The fiber is pumped by a 980 nm multi-mode laser diode via a multi-mode combiner (MMC). A polarization controllers (PC) is used to adjust the polarization state of the oscillating light and the birefringence inside the ring cavity. An isolator is incorporated in the laser cavity to ensure unidirectional propagation of the oscillating laser as well as to function as an artificial SA when combined with the intra-cavity birefringence. The light is coupled out of the cavity by a 95/5 fiber coupler. In order to avoid passive mode-locking, it is worth noting that we intentionally use a 95/5 coupler, which allow only 5 % of the light to oscillate in the cavity. This induces a cavity loss of more than 15 dB in the laser cavity, which is sufficient enough to avoid mode-locking. The total cavity length of the ring resonator is measured to be around 10 m. When the pump power is above the threshold, stable Q-switching pulse is generated when the PC is adjusted in such a way so that the light could not oscillate in the cavity as there is no feedback. At the same time, population inversion builds up leading to high stored energy in the gain medium. After some time the gain medium will be saturated and amplification will take place where Q-switch pulse is formed. The optical spectrum analyzer (OSA) is used to inspect the output spectrum of the Q-switched EYDFL whereas the oscilloscope is used to observe the output pulse train via a 1.2 GHz bandwidth photo-detector.

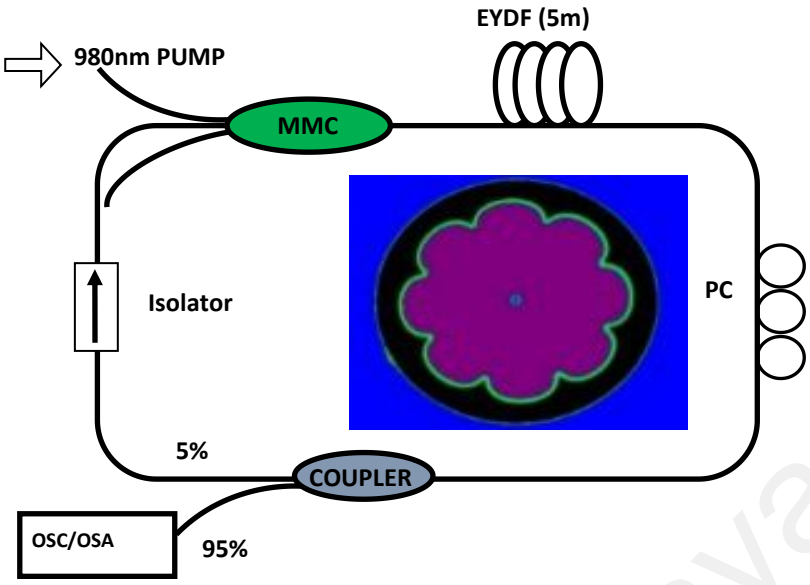

Figure 3.1: Schematic diagram of the proposed Q-switched EYDFL based on NPR technique. Inset shows a cross-section image of the EYDF with a multi lobed pump guide structure.

In our experiment, NPR technique was applied to implement Q-switching operation. The combination of PC and polarization dependent isolator acted as an artificial saturable absorber due to the NPR effect so that the intensive waves transmitted in the laser cavity while the weak ones were suppressed. During the process of experiment, when the pump power was increased to about 300 mW, the fiber laser can be easily tuned to operate in the Q-switching state via appropriately adjusting the PC. The optical spectrum and temporal waveform of the laser beam is shown in Figures 3.2 (a) and (b), respectively at pump power of 500 mW. As shown in Figure 3.2 (a), the EYDFL operates at 1543.51 nm with a 3 dB bandwidth of 0.27 nm. The spectral broadening is observed in the spectrum due to self-phase modulation (SPM) effect in the laser cavity. The pulses were sequenced in a train uniformly at the pulse separation of 21.1 μs, which corresponds to repetition rate of 46.95 kHz at this pump power as shown in Figure 3.2 (b). The pulse width of the pulse train is measured to be around 5.3 μs.

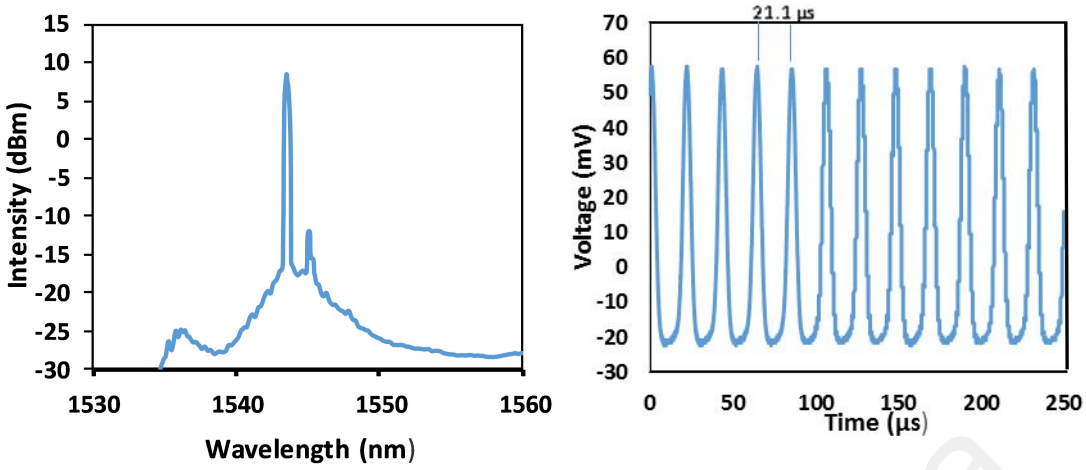

(a) (b)

Figure 3.2: The spectral and temporal characteristics of the proposed Q-switched EYDFL (a) optical spectrum (b) typical pulse train at the pump power of 500 mW.

By adjusting the polarization state of the oscillating light with the help of PC, the Q-switching pulse is obtained within the pump power range from 300 to 600 mW. The pump laser creates population inversion in the fiber. As soon as the Erbium ions reach excited state through non radiative energy transfer from Ytterbium ions, some of them undergo spontaneous emission and a fraction of this is guided by the EYDF. Due to the presence of a large number of longitudinal modes which have in general random phase relationships with each other, the light intensity within the ring will have fluctuations. If we consider a portion of light intensity within the ring just before the polarization controller it is linearly polarized and the PC changes it into some elliptical polarization state. If we assume that the fibers within the ring maintain the polarization state, then as oscillating light corresponding to low intensity will not be able to pass through the PC as it is adjusted to block the propagation of the elliptically polarized light. Now consider a short pulse of high intensity fluctuations arising out of the interference between various longitudinal modes as it starts from the right end of the fiber, it is linearly polarized and can pass through the PC converted to an elliptically polarized light after losing a portion of light at the output probe of the coupler the rest of

the light passes through the isolator and MMC enters the EYDF where it undergoes nonlinear polarization rotation and recovers its linear polarization state, which will employ low loss for the high intensity portion. At the same time the low intensity portion of the pulse will not undergo polarization rotation and thus would be partially blocked by the PC. Hence ring is exhibiting low losses (high Q) for high intensity portion and high losses (low Q) for low intensity portion. This in turn will ensure that the high intensity portions grow in intensity, while the low intensity portions die out, resulting in the generation of pulses with high energy. Thus the phenomenon of non-linear polarization leads to the generation of high energy pulses.

It comes to our attention that the repetition rate and pulse width of the Q-switched pulses is sensitive to the pump power. In order to further investigate the relationship between them, we fastened the direction of PC, and increased the pump power from 300 to 600 mW. It is observed that the Q-switching pulse disappears as the pump power is increased above 600 mW. The dependence of the repetition rate and pulse width on the input pump power is shown in Figure 3.3. As shown in the figure, the repetition rate increases almost linearly with the pump power. The result coincides well with the inherent characteristic of the Q switched fiber laser as reported before (Yap et. al., 2012). The pulse repetition rate can be varied from 26.7 to 70.08 kHz as the pump power increases from 300 and 600 mW. On the other hand, the pulse width decreases from 7.5 to 5.3 μs as the pump power increases from 300 to 500 mW. However, with further increase in pump power, the pulse width increases to 6.62 μs at 600mW as shown in Figure 3.3. This is attributed to the increased phase noise in the cavity.

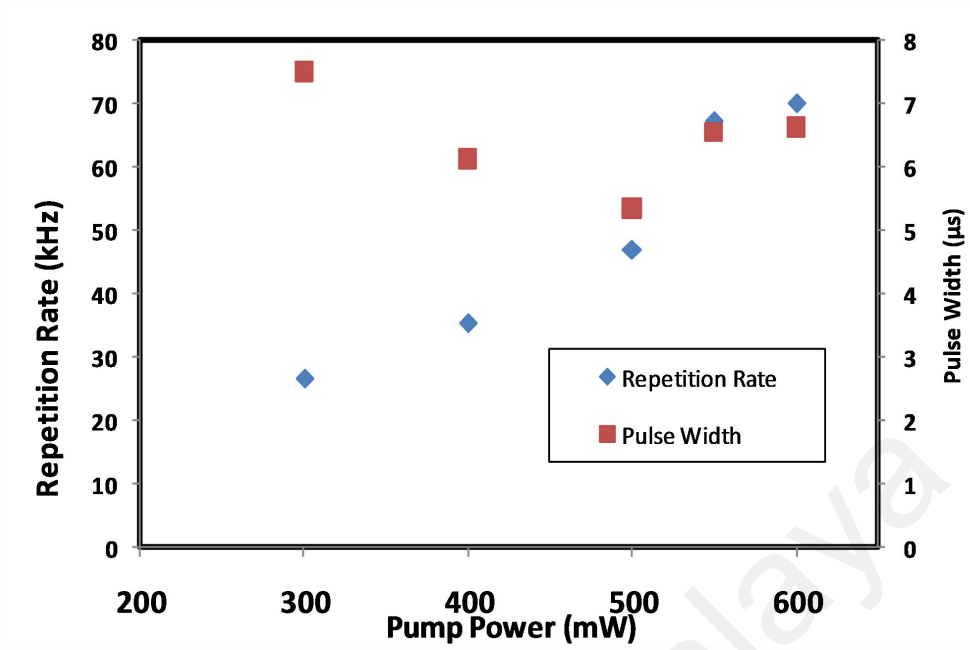

Figure 3.3: Repetition rate and pulse width as functions of 980 nm multi-mode pump power.

Figure 3.4 shows the pulse energy and average output power of the Q-switched EYDFL as functions of pump power. Both output power and pulse energy show an increasing trend with the pump power. As shown in the figure, the Q-switched laser has a slope efficiency of 1.39 % with the maximum output power of 5.23 mW is obtained at 600 mW multi-mode pump power. On the other hand, the pulse energy increases from 48.7 to the maximum value of 75.6 nJ as the pump power increases 300 to 500 mW. However, the pulse energy starts to saturate as the pump power further increases. Figure 3.5 shows the radio frequency (RF) spectrum of the Q-switched EYDFL, which was obtained using RF spectrum analyzer via a 1.2 GHz photo-detector. As shown in the figure, the repetition rate is obtained at 46.95 kHz with signal to noise ratio of about 50 dB, which indicates the stability of the Q-switched laser. The harmonics of the Q-switching frequency are present because the modulation of the laser output at the Q-switching frequency is far from sinusoidal. These results indicate that NPR technique has a big potential for Q-switching applications using just simple configuration with

cladding pumping. This inexpensive laser is suitable for applications in metrology, environmental sensing and biomedical diagnostics.

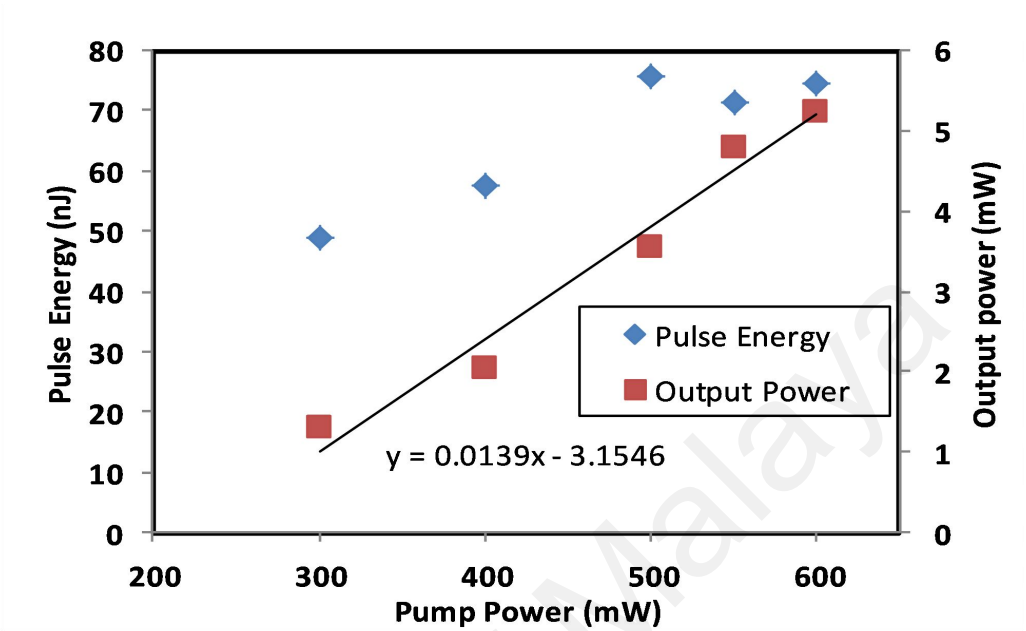

Figure 3.4: Pulse energy and average output power as functions of 980 nm multi-mode pump power

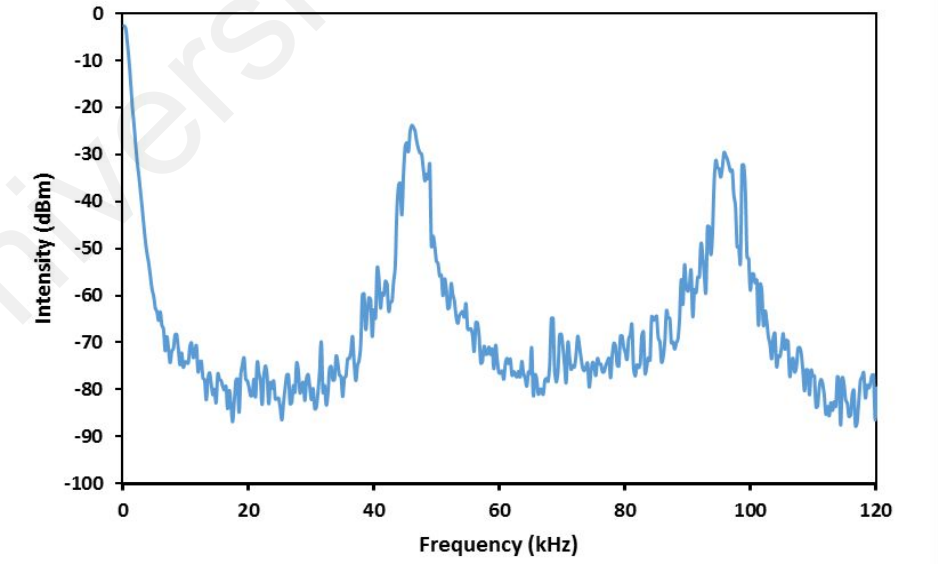

Figure 3.5: RF spectrum of the Q-switched EYDFL at pump power of 500 mW.

3.3 Dual-wavelength passively Q-switched fiber laser based on NPR

The multi-wavelength Q-switched lasers, which can simultaneously generate synchronized Q-switched pulse trains at different centre wavelengths, can be useful in airborne Lidar, terahertz generation, multi-photon dissociation of molecules and other nonlinear optics or sensing applications (Anyi et al., 2013; Dong et al., 2012). Very recently, by using the birefringence-induced filtering effect, a dual-wavelength Q-switched EDF laser with a graphene saturable absorber (Luo et al., 2010) and single-walled carbon nanotubes (Liu et al., 2013) have been reported. In this section, a dual-wavelength Q-switched EYDFL is proposed and demonstrated based on the NPR technique by configuring the laser cavity so that it has sufficiently high loss to prevent mode locking. The schematic of our dual-wavelength Q-switched EYDFL is shown in Figure 3.6. The fiber laser is constructed using a simple ring cavity, which uses similar components with the previous experiment of Figure 3.1. The setup is almost similar except for the incorporation of two PC in the cavity instead of one in the single-wavelength configuration. Two PCs are used to adjust the polarization state of the oscillating light and the birefringence inside the ring cavity.

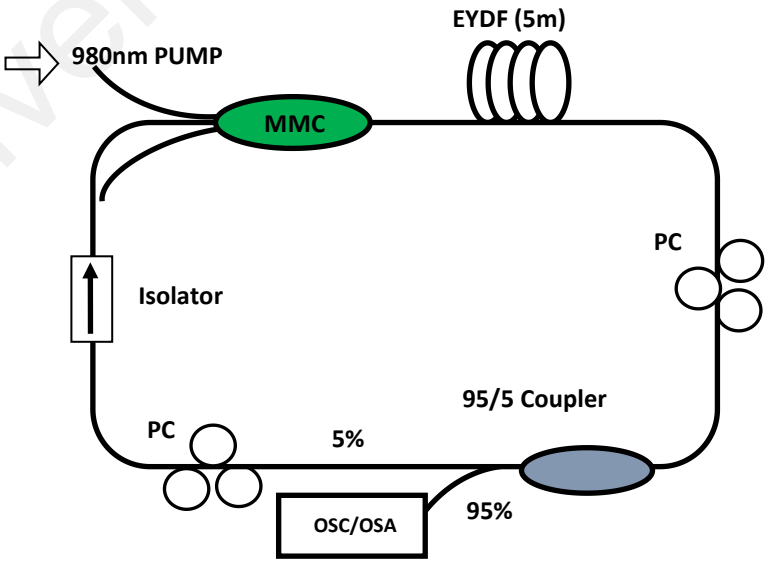

Figure 3.6: Schematic diagram of the proposed dual-wavelength Q-switched EYDFL based on NPR technique.

In this experiment, NPR technique was applied to implement both dual-wavelength and Q-switching operations. The NPR provides an intrinsic feature of the spectral filtering effect and thus it is possible to obtain multi-wavelength laser by using the NPR technique. By adjusting the polarization in the ring-cavity, NPR can induce intensity dependent loss to suppress the mode competition caused by homogeneous broadening in EYDF. As the pump power was more than 0.27 W, dual-wavelength Q-switched lasing was shown. Moreover, the dual wavelength operation maintained with the enlargement of the pump power. An OSA with a wavelength resolution of 0.05 nm was used to capture the output laser spectrum. Figure 3.7 shows the measured spectrum of dual wavelength Q-switched lasing under pump power of 0.60 W. The wavelength separation of the output spectrum is 2.1 nm and the laser bandwidth is about 0.08 nm. It is also observed that the signal to noise ratio of 1543.3 nm and 1545.4 nm lines are obtained at 15 dB and 18 dB, respectively. Note that the channel spacing depends on cavity birefringence, which can be tuned by rotating the PC.

The combination of PC and isolator acted as an artificial saturable absorber due to the NPR effect so that the intensive waves transmitted in the laser cavity while the weak ones were suppressed. During the process of experiment, when the pump power was increased to about 0.27 W, the fiber laser can be easily tuned to operate in the Q-switching state via appropriately adjusting the PC. The temporal waveform of the laser beam is shown in Figure 3.8 at pump power of 0.27 W. As shown in Figure 3.8 (a), the pulses were sequenced in a train uniformly at the pulse separation of 82.9 μs, which corresponds to repetition rate of 12.06 kHz at this pump power. The pulse width of the pulse train is measured to be around 11.56 μs as shown in Figure 3.8 (b). Note that the pulses at the two wavelengths have the same repetition rate, and, as the pump power increases, both repetition rates increase.

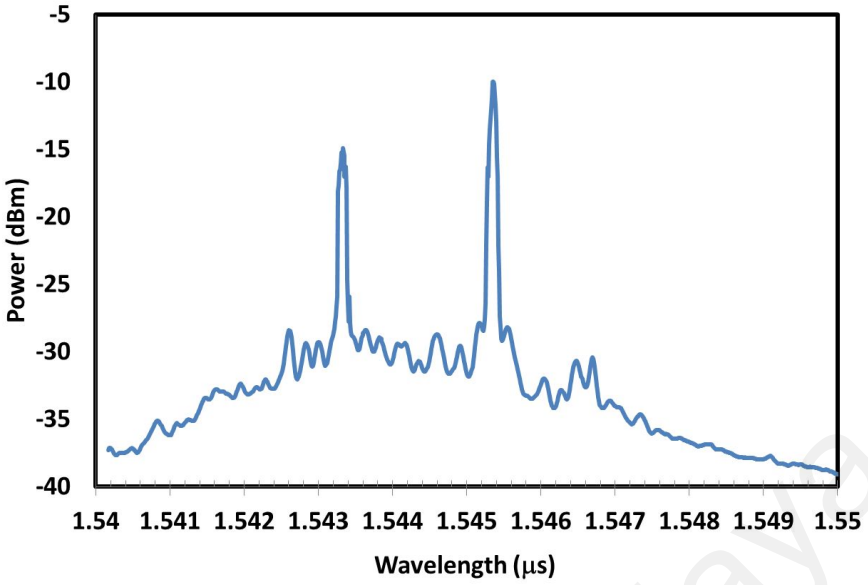

Figure 3.7: Output spectrum of the dual wavelength Q-switched EYDFL at pump power of 0.60W.

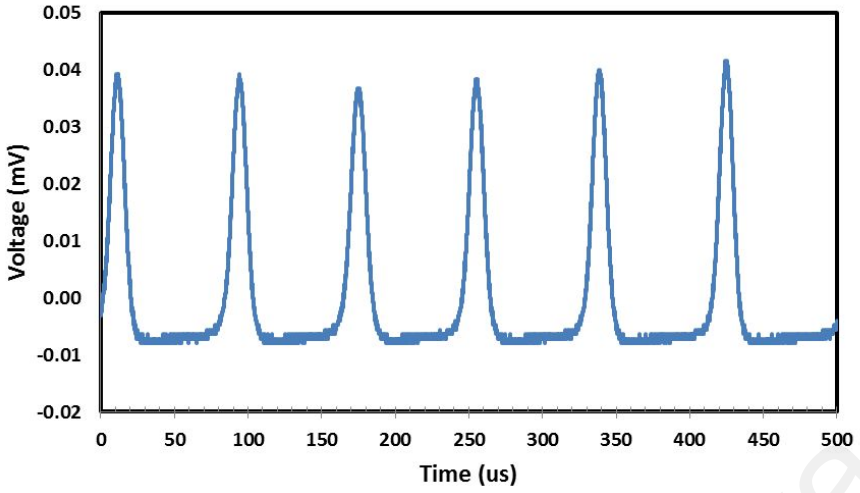

(a) Typical pulse train

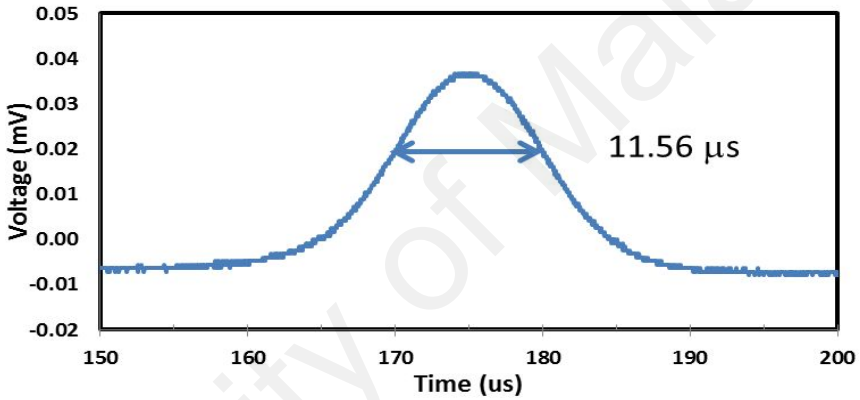

(b) Single pulse envelop

Figure 3.8: The temporal characteristic of the dual-wavelength Q-switched EYDFL (a) typical pulse train and (b) single pulse envelop at the pump power of 0.27 W.

The pulse repetition rate and pulse width of the Q-switched laser are shown in Figure 3.9 at varying pump powers. Similar with many other passively Q-switched lasers, the repetition rate is closely related to the pump level: the higher the pump power, the higher the repetition rate is. That is because high pump power leads to a shorter time for the inversion number of the gain medium to reach the threshold. It is observed that the repetition rate of the Q-switched EYDFL can be tuned from 12.06 kHz to 57.94 kHz by varying the multi-mode pump power from 0.27 W to 0.60 W. As indicated in the previous work, the long pulse duration of ~µs is due to the long cavity lifetime related to

the long length of the cavity, which can be reduced by decreasing the cavity length with a highly doped Erbium fiber or other more compact components. In our experiment, we observe that the pulse duration of the Q-switched laser reduces from 11.56 µs to 5.04 µs as the pump power increases from 0.27 W to 0.55 W. However, the pulse width is slightly increased at the maximum pump power of 0.60 W.

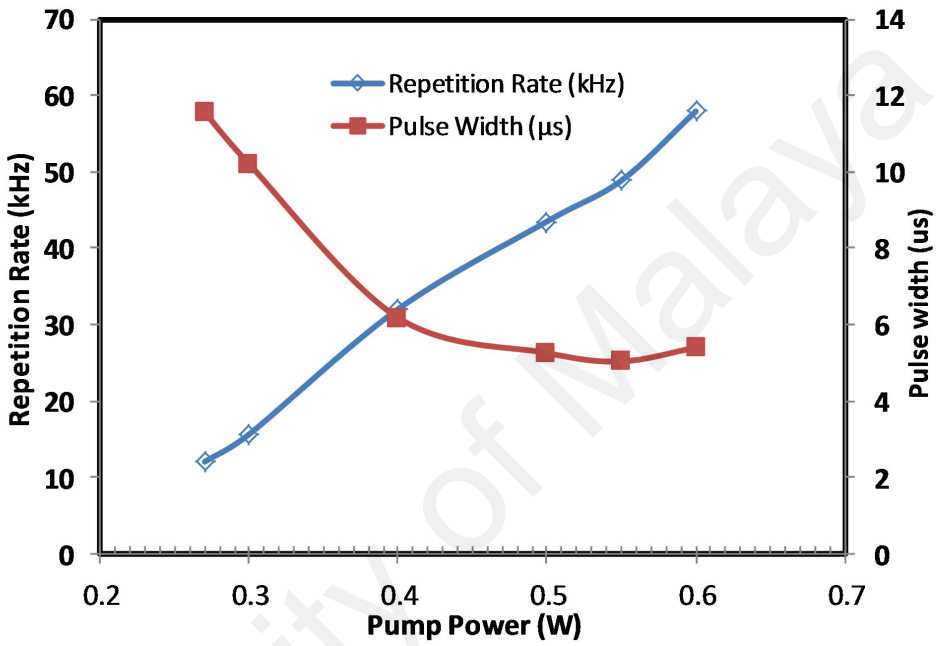

Figure 3.9: Repetition rate and pulse width as functions of 980 nm multi-mode pump power.

Because of the slightly higher gain at the longer wavelength of 1545.4 nm, the pulses at this wavelength have a higher peak power and energy in the cavity, compared to those at 1543.3 nm. Figure 3.10 shows the relationship between the pulse energy and peak power of the dual-wavelength Q-switched laser against the pump power for 1545.4 nm line. Both pulse energy and peak power increase with the increment of pump power from 0.27 W to 0.55 W. However, both energy and peak power are slightly degraded as the pump power is further increased to 0.60 W due to saturation effect. The maximum pulse energy and peak power are obtained at 72.01 nJ and 13.4 mW, respectively when the pump power was 0.55 W.

Figure 3.11 shows the radio frequency (RF) spectrum of the Q-switched EYDFL, which was obtained using RF spectrum analyzer via a 1.2 GHz photo-detector. The pump power is fixed at 0.60 W. As shown in the figure, the repetition rate is obtained at 57.94 kHz with the signal to noise ratio of about 25 dB, which indicates the stability of the Q-switched laser. These results indicate that NPR technique has a big potential for both dual wavelength and Q-switching applications using just simple configuration with cladding pumping. This inexpensive laser is suitable for applications in metrology, environmental sensing and biomedical diagnostics.

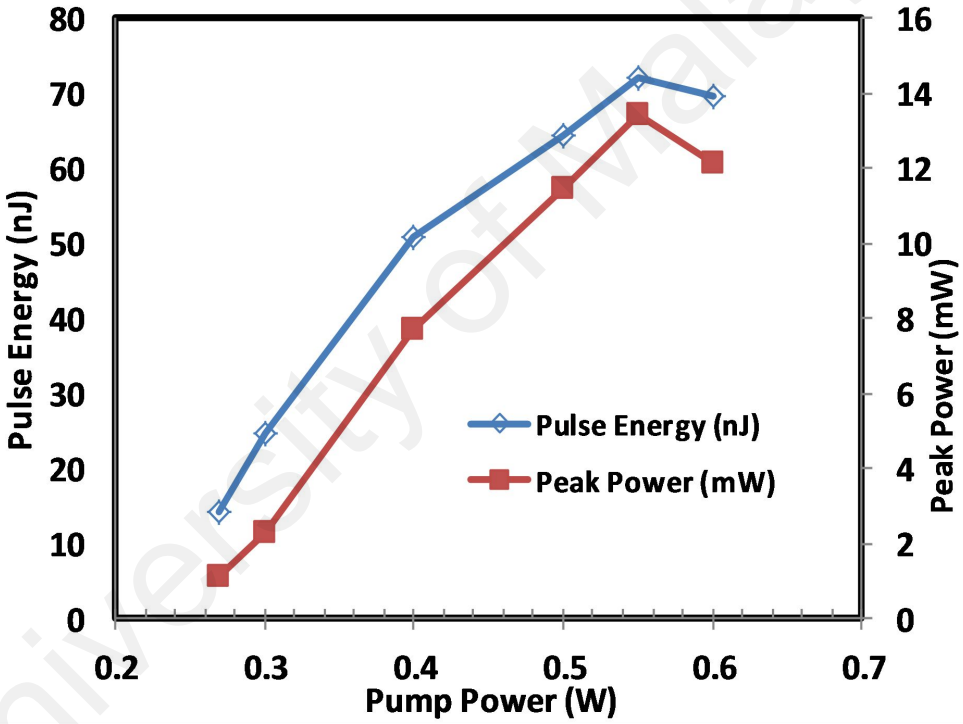

Figure 3.10: Pulse energy and peak power as functions of 980 nm multi-mode pump power.

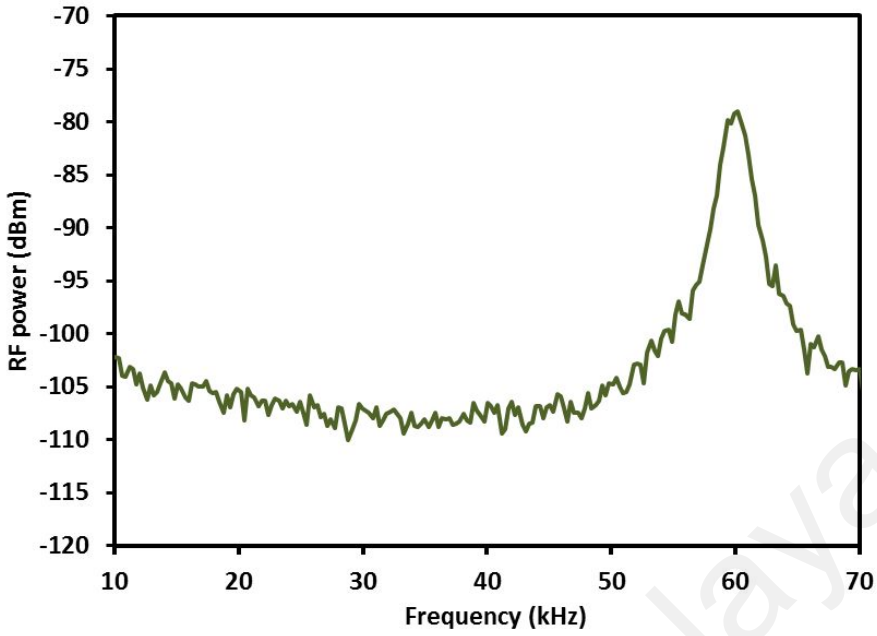

Figure 3.11: RF spectrum of the dual-wavelength Q-switched EYDFL at pump power of 0.60 W.

3.4 Summary

The Q-switched cladding pumped EYDFL has been demonstrated using a NPR technique to operate at 1543.5 nm. It employs an isolator in conjunction with a highly nonlinear EYDF to induce intensity dependent loss in a sufficiently-high loss ring cavity and thus generates a Q-switching pulse at threshold pump power as low as 300 mW. At 980 nm multi-mode pump power of 500 mW, the EYDFL generates a sequence of pulses with a repetition rate of 46.95 kHz, pulse width of 5.3 μs and the maximum pulse energy of 75.6 nJ. When the multi-mode pump power is varied from 300 to 600 mW, the repetition rate can be tuned from 26.7 to 70.08 kHz while the pulse width fluctuates within 7.5 to 5.3 μs. The dual-wavelength Q-switched cladding pumped EYDFL has also been demonstrated by incorporating an additional PC in the ring cavity. The proposed NPR-based dual-wavelength laser operates at 1543.3 nm and 1545.4 nm and the Q-switching pulse has been achieved at threshold pump power as low as 0.27 W. When the multi-mode pump power is varied from 0.27 to 0.60 mW, the EYDFL generates a sequence of pulses with repetition rate that can be tuned from 12.06 kHz to

57.94 kHz and the pulse width that fluctuates within 11.56 μs to 5.04 μs. The lowest pulse width of 5.04 μs and the maximum pulse energy of 72.01 nJ are obtained at the pump power of 0.55 W.

Chapter 4

Q-switching and Mode-locking Pulse Generation with Graphene Oxide Paper Based Saturable Absorber

4.1 Introduction

Pulse fiber lasers have great potential applications in fields such as spectroscopy, biomedical diagnoses, fiber communication and so on (Anyi et al., 2013; Q. Wang et al., 2013). Up to date, most of the pulse fiber lasers have adopted passive technique, in which saturable absorbers (SAs) act as a key part. The improvement of lasers relies on the optical properties of SAs, for instance, transparency and optical non-linearity. There have been attempts on several types of SAs materials. Semiconductor SA mirrors (SESAMs) currently dominate passive Q-switching and mode-locking (Keller, 2003; Zhipei Sun et al., 2010; J. Wang et al., 2012). However, some intrinsic disadvantages of SESAMs still remain, such as limited operation bandwidth and complex fabrication/packaging. As a promising SAs candidate, single walled carbon nanotubes (SWCNTs) have advantages both in recovery time and saturable absorption (Martinez et al., 2013; Set et al., 2004). In order to achieve waveband tuning, SWCNTs with different diameters have to be mixed, resulting in extra linear losses, consequently increasing the difficulty of mode locking. As an up and coming material in recent years, graphene possesses favorable characteristics for SAs, similar to SWCNTs. As a result of gap less linear dispersion of Dirac electrons, graphene SAs would achieve wideband, tunable operation without the need of bandgap engineering or chirality/diameter control. (Bonaccorso et al., 2010; Popa et al., 2010; Ugolotti et al., 2012). However, the processability are the first issue for the graphene based materials.

Graphene oxide (GO), an example of chemically treated graphene, has also attracted much attention recently as a potential alternative to graphene (Dikin et al., 2007). The structure of GO is composed of sp^2-bonded areas with variable size, which are divided by surface oxidation in the form of carboxyl, hydroxyl or epoxy groups. The synthesis of GO is relatively easier than graphene, and more importantly, can be prepared in large quantities in both water and organic solvents (Dikin et al., 2007; Zhu et al., 2010). Although the electric conductivity is highly influenced by the content of defect clusters, GO has good optical properties. Further investigation shows GO has ultra-fast recovery time and strong saturable absorption, which is comparable to that of graphene (Loh et al., 2010; C. Zhao et al., 2012). Many research works on pulse fiber lasers have also been demonstrated using the GO as a saturable absorber. The GO based SAs are realized by many techniques such as mirror (Xu et al., 2012), photonic crystal fiber filled with few-layered graphene oxide solution (Liu et al., 2011), fused silica windows with GO and reduced GO layers (Sobon et al., 2012), GO aqueous dispersion (J. Wang et al., 2012), reflective GO absorber with glass and copper (Feng et al., 2012), sandwich structured GO/PVA absorber (K. Wang et al., 2013) and GO membrane on microfiber (He et al., 2012).

Recently, a graphene oxide paper has also been developed and commercially available for various applications. It can be prepared by mixing graphite oxide in water. The oxygen atoms of graphite oxide repel water molecules, thus, undergoing complete exfoliation in water, producing a colloidal suspensions of almost entirely individual graphene oxide sheets. After filtering the exfoliated mixture through a membrane, these graphene oxide sheets could be made into paper-like material under a directional flow. A free-standing graphene oxide paper is obtained after drying. By changing the oxygen amount on the layers, the material can be an electrical insulator, semi-conductor or conductor. This material is uniform and dark brown in colour (Dikin et al., 2007).

In this chapter, various pulse fiber lasers are demonstrated using a commercially available non-conductive graphene oxide paper as a saturable absorber. The easy fabrication of graphene oxide paper will promote its potential in Q-switching and mode-locking applications.

4.2 Preparation of Graphene Oxide Saturable Absorber (GOSA)

GOSA used in this experiment is based on Graphene Oxide paper purchased from graphene supermarket at a comparable low price due to its simpler manufacturing process with mass production and has an advantage in terms of mechanical properties (Dikin et al., 2007; Zhu et al., 2010). Similar to graphene SA, the implementations of GOSA is simple by just deposit or attach the GO paper into the laser path at one end of the fiber ferrule surface. A common method used to deposit graphene on the fiber ferrule surface is by using optical radiation attraction method (Z. Luo et al., 2010). This method is used due to the sheet size of the graphene is too small (typically lateral dimension of 100 nm to few microns in length (Dong et al., 2010) to hold and attach to the fiber end surface. GO is however different, the sheet size of the GO is compatibility larger (typically lateral dimension of few tens of microns up to few hundreds of microns (N. Huang et al., 2011) making it much easier to handle. Large lateral sheet size GO is chosen to assemble the GOSA in this experiment as it is able to pick up using a laboratory tweezers and place on the fiber ferrule surface directly. To ensure that the GO paper stick and maintain its position at the centre of the fiber ferrule of a connector, small volume of index matching gel is place at the centre of the fiber ferrule that covers the fiber core or the laser path. When the GO paper is in contact with the index matching gel at the fiber ferrule, it will stick and attach to the fiber ferrule and cover the fiber end surface. Figure 4.1 shows the microscopic image of the GO paper that attached

at the centre of fiber ferrule covering the laser path with index matching gel surrounding it. The connector will later connect with another connector via FC/PC adapter to sandwich the GO paper to avoid major displacement and form the required SA.

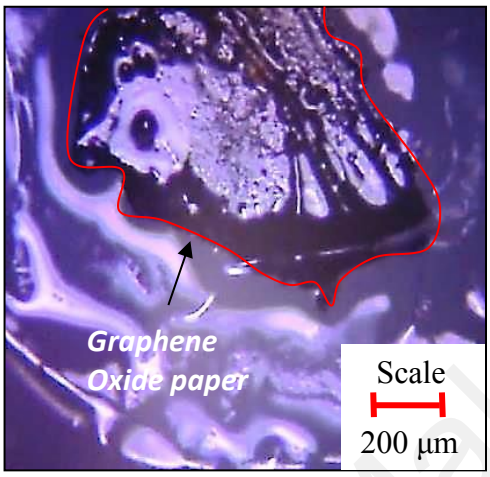

Figure 4.1: Microscopic image of GO paper surrounded by index matching gel. The GO paper sits at the centre of the inner section covering the fiber core.

The Raman Spectroscopy which is widely used to characterize crystal structure, disorder and defects in graphene-based materials is used for the same purpose in this work. A 50 mW laser at wavelength 532 nm was radiated on the GO paper for a duration of 10 s to generate Raman emission from the GO paper. The Raman spectrum obtained from the Raman Spectroscopy scanning is shown in Fig 4.2. For reduce graphene oxide (rGO) and GO, they always refer to two important bands which name as the D (for Defect) and G (for Graphite) band. The D band represents the disorder breaks of the crystal symmetry of carbon sp^2 rings which leads to certain vibrational modes (Ado et al., 2011). It is common to all sp^2 carbon lattice and arises from the stretching of C-C bond which cause by the O-incorporation (Sobon et al., 2012). While the G band represents the first order scattering of the E_{2g} phonon of sp^2 C atoms (Ferrari et al., 2000). The peaks of D and G bands of GO normally located around 1352 cm^{-1} and

1585 cm^{-1}, but it is found to be at approximately 1353.00 cm^{-1} and 1585.35 cm^{-1} respectively in Figure 4.2.

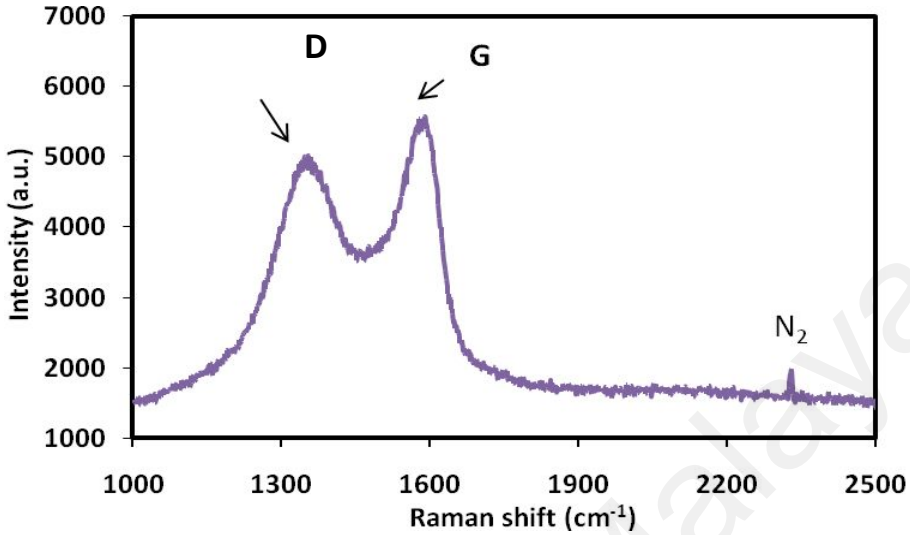

Figure 4.2. Raman spectrum of GO paper measured using Renishaw Raman Spectroscopy.

As the D band represents the disorder breaks of the crystal symmetry of carbon sp^2 rings, hence the graphitic edge which related to the GO size will also contributed to the intensity of D band. The smaller the size of the GO sheets, the higher the peak of the D band. The relative intensity ratio of both D and G peaks (I_D/I_G) is a measure of disorder degree and is inversely proportional to the average size of the sp^2 clusters which is 0.8971. Although there are disordered cause by the O-incorporation that raise the D peak, however the D peak is still relatively low due to the large GO sheets that close to lateral size of few hundreds micron which applied on the fiber end as shown in Figure 1. The small peak at 2329 cm^{-1} is the N_2 peak which indicates the presence of ambient nitrogen gas. In Figure 2, 2D band which normally used to distinguish the thickness and doping level of the graphene sheets was not observed. This is most

probably due to the laser power, which is low as well as the contribution of unintentional doping including O_2 (S. Zhao et al., 2012).

4.3 Q-switched Erbium-doped fiber laser with GO paper as SA

Figure 4.3 shows the experimental setup of the proposed Q-switched Erbium-doped fiber laser (EDFL) using a ring configuration with a GOSA. A 0.8 m long EDF is used as gain medium to provide an amplified spontaneous emission (ASE) at C-band by pumping it with a 980 nm laser diode through a wavelength division multiplexer (WDM). An isolator is used to ensure unidirectional light propagation and the stability of the generated laser. In order to generate Q-switching pulse train, a GOSA assembly is placed inside the laser cavity as a Q-switcher. A 10 dB coupler is used to tap out 10% of the laser light from the ring cavity. In order to make accurate measurements, a 3dB coupler is used to split the laser power into two, where one channel is fixed to a high resolution optical spectrum analyzer (OSA) to monitor the laser output spectrum while the other channel to measure either average output power, time domain, and radio frequency spectrum.

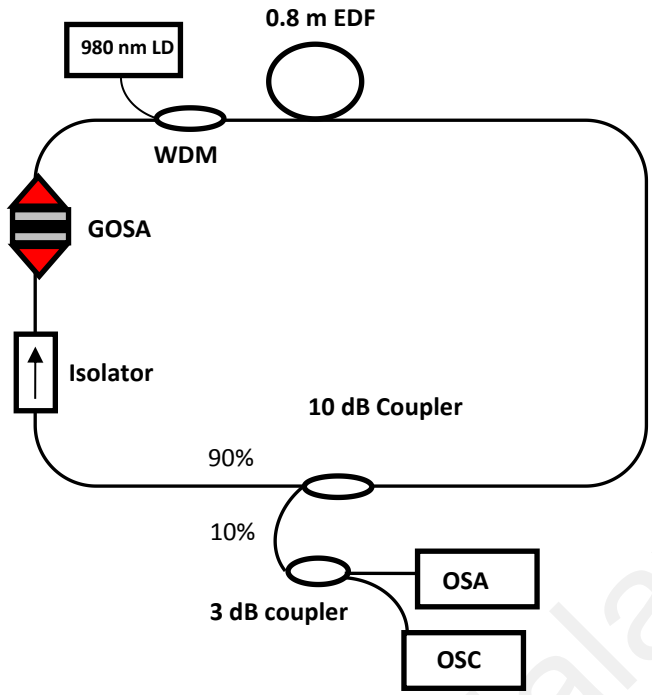

Figure 4.3: The configuration of the proposed Q-switched EDFL

Initially, the continuous wave (CW) EDFL was investigated without putting the GOSA and the laser threshold was found to be at the pump power of 18 mW. It should be noted that no Q-switched operation occurs without the GOSA connected in the laser cavity. It is clear that the Q-switched operation is mainly induced by the SA. However, a stable and self-starting Q-switched operation was only observed at the pump power of 22 mW. Figure 4.4 shows the optical spectrum of the Q-switched laser at 980 nm pump power of 22 mW. It operates at 1534.4 nm with a signal to noise ratio of more than 25 dB. For the purpose of comparison, we have also shown the CW lasing spectrum in Figure 4 with dashed curve. As can be seen in Figure 4.4, the spectrum of the Q-switched operation has a larger bandwidth than that of CW lasing operation. This might due to the self-phase modulation effect in the laser cavity. It is also observed that the operating wavelength of the laser shifted from 1557.7 nm to 1534.4 nm with the incorporation of GOSA. This is attributed to the cavity loss, which increases with the incorporation of SA. Therefore, the laser operates at a shorter wavelength to acquire

more gain to compensate for the loss. Correspondingly, the typical Q switched pulse train is presented in Figure 4.5 when the pump power is fixed at 50.5 mW. The repetition rate is 31.5 kHz. The pulse duration, which was measured directly from an oscillograph, is about 13.8 μs. The figure also shows no distinct amplitude modulation in each Q-switched envelop spectrum. This indicates that the self-mode locking effect on the Q-switching is weak for the proposed laser.

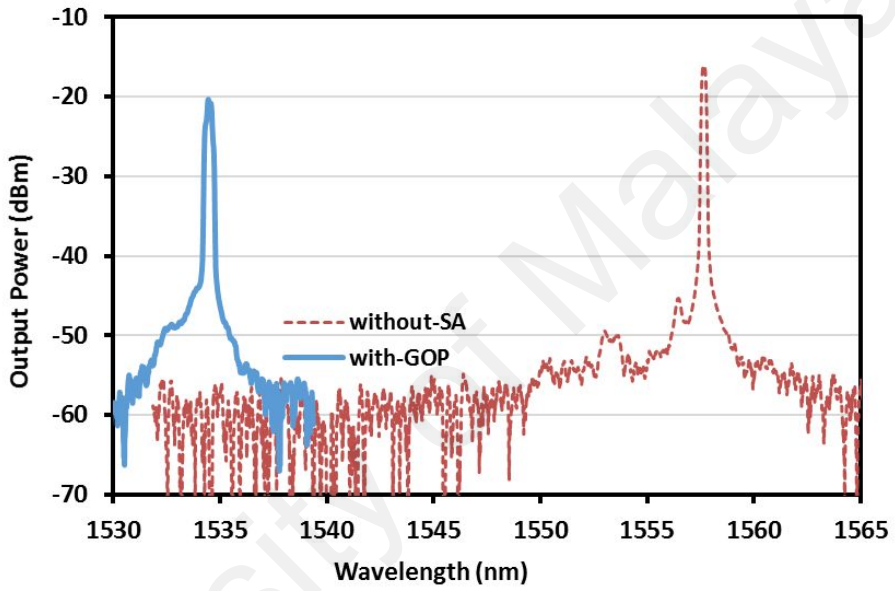

Figure 4.4: Output spectra of the EDFL with and without the GOSA. Inset shows the typical Q-switching pulse train with the GOSA at pump power of 50.5 mW.

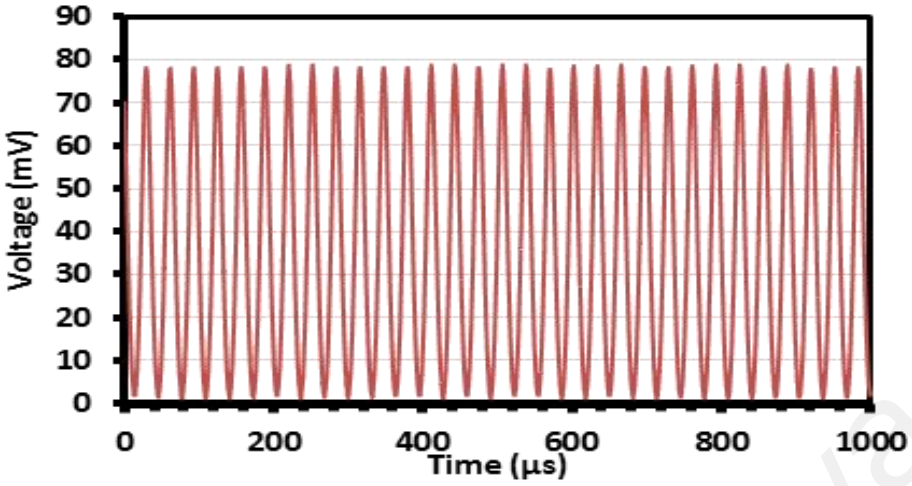

Figure 4.5: Typical pulse train for the Q-switched EDFL with GOSA

We then measured the tuning range of the Q-switched output pulse as a function of pump power. As shown in Figure 4.6, the output pulse width and repetition rate changed when the pump power increased. Like typical Q-switched fiber lasers, the pulse repetition rate increases from 14.3 to 31.5 kHz with increasing pump power from 22.0 to 50.5 mW. On the other hand, the pulse width decreases from 32.8 to 13.8 µs as the pump power is increased within the same range. This effect is due to gain compression in the Q-switched fiber laser. Further reduction in pulse width is expected by shortening the cavity length using a higher dopant fiber. Figure 4.7 shows the RF spectrum of the Q-switched laser at pump power of 50.5 mW. It shows that the laser operates at a repetition rate of 31.4 kHz with a signal to noise ratio of around 12 dB. This indicates the stability of the pulse train generated by the proposed Q-switched EDFL. It is worthy to note that the Q-switching pulse disappears as the pump power is further increased above 50.5 mW.

Figure 4.8 shows the average output power and pulse energy of the Q-switched EDFL as functions of pump power. As shown in the figure, the average output power

increases from 0.11 mW to 0.48 mW while the pulse energy fluctuates within 7.7 nJ to 16.8 nJ as the pump power increases from 22.0 to 50.5 mW. The maximum pulse energy of 16.8 nJ is obtained at the pump power of 45.5 mW. We believe that the pulse energy could be improved by reducing the insertion loss of the GOSA and optimizing the laser cavity.

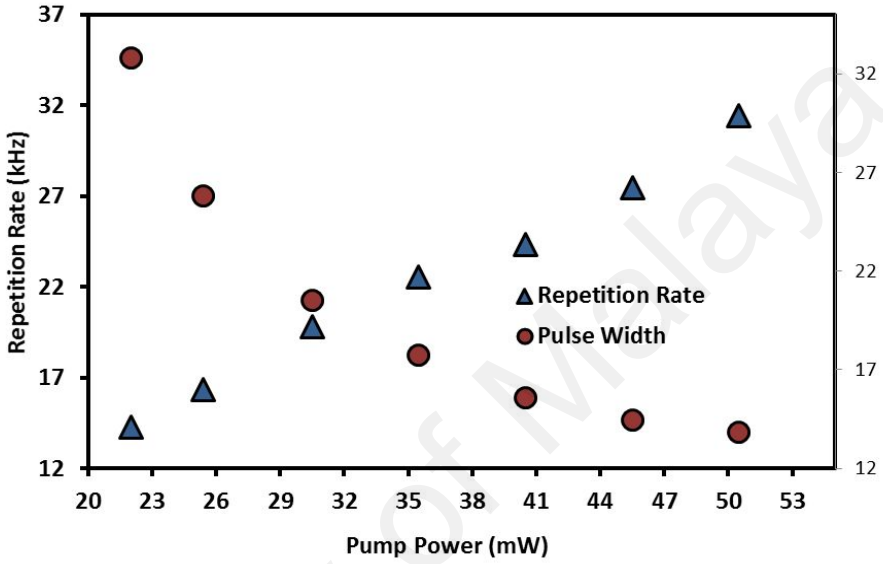

Figure 4.6 : Repetition rate and pulse width as a function of 980 nm pump power. Inset shows the RF spectrum of the Q-switched laser at pump power of 50.5 Mw

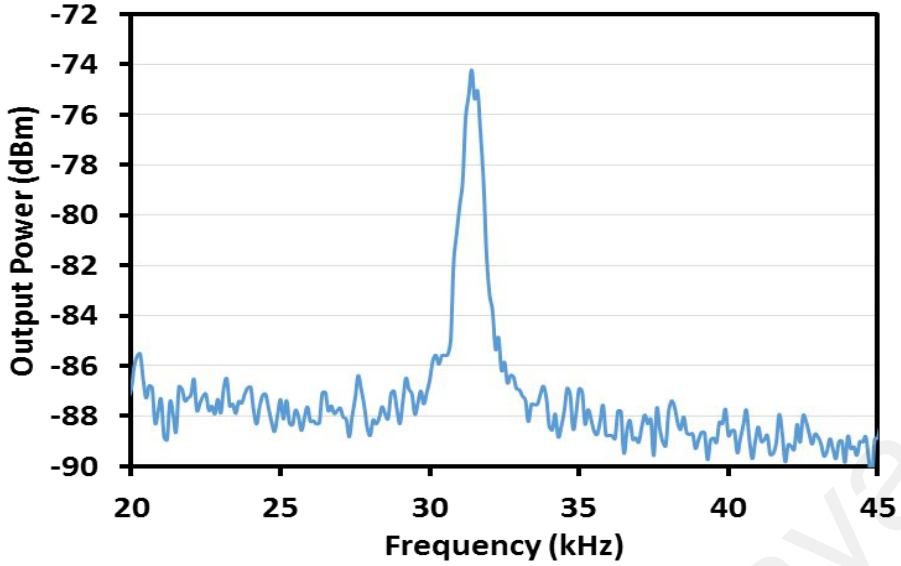

Figure 4.7: RF spectrum of the Q-switched laser at pump power of 50.5 mW.

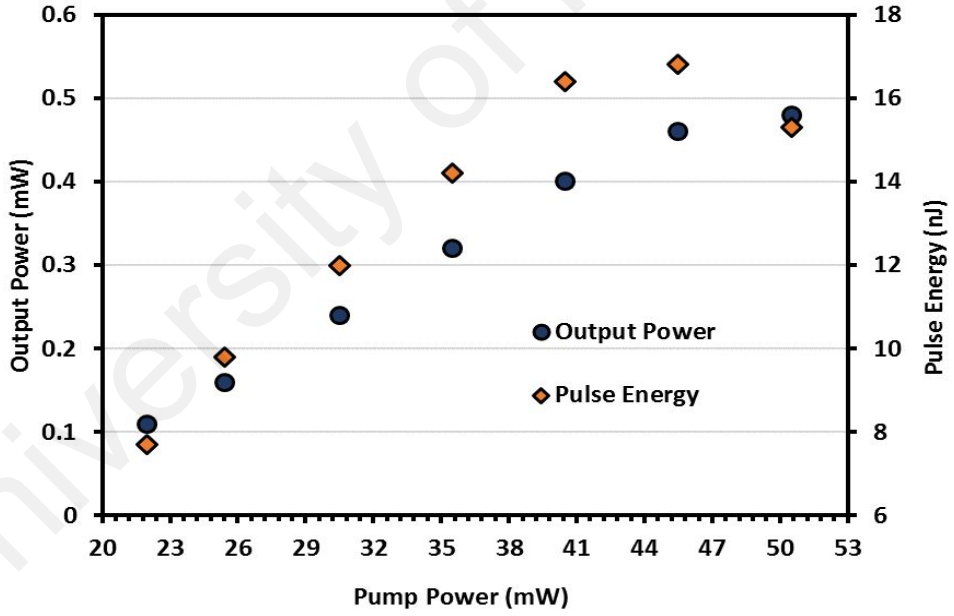

Figure 4.8: Average output power and pulse energy as a function of 980 nm pump power

4.4 Dual-wavelength Q-switched EDFL

Many works on all-fiber dual-wavelength fiber lasers have also been reported in recent years due to interests in their potentials in applications such as optical instrument testing, optical signal processing, fiber sensing systems and microwave photonics. For instance, a dual wavelength Q-switched fiber lasers was reported by Luo et. al. (Luo et al., 2010) in 2010. In this section, a dual wavelength Q-switched EDFL with a very narrow wavelength spacing of 33 pm is demonstrated by using a GO paper as saturable absorber. A tunable band pass filter (TBF) and a short length of photonics crystal fiber (PCF) are utilized in the cavity to produce the dual wavelength fiber laser via Four-Wave-Mixing (FWM) effect.

Figure 4.9 shows the experiment setup of a dual-wavelength Q-switched EDFL, which uses a 3 m long EDF as gain medium. By pumping the EDF with a 980 nm laser diode through a WDM, an amplified spontaneous emission (ASE) is generated at C-band, which oscillates in the ring cavity to generate laser. Two isolators are used in the ring cavity to ensure unidirectional light propagation and the stability of the generated laser. A PCF is used to generate a stable and narrow spacing dual-wavelength laser by polarization dependence loss (PDL) and fringe spacing effects, where its terminals are mechanical coupled with SMF-28 fiber via the bare fiber holders. In the inset of Figure 4.9, a microscopic picture of the PCF's cross section is shown, having holes with diameter of 5.06 μm and the distance between the centre of each hole is 5.52 μm. It has a core diameter of 4.37 μm and a fiber diameter of 124 μm. In order to generate dual-wavelength laser, the polarization controller (PC) is adjusted accordingly to switch the laser polarization states to a proper state. In addition, a TBF with a band pass bandwidth of 0.8 nm and tuning resolution of 0.05 nm is employed into the laser cavity to filter the unwanted laser emissions, and band pass the required dual-wavelength laser. By carefully fine tune the TBF and PC, a narrow spacing dual-wavelength laser is obtained.

A GOSA assembly is then placed inside the laser cavity as a component to generate the Q-switched dual-wavelength laser. A 10 dB coupler is used to tap out 10% of the laser light from the ring cavity.

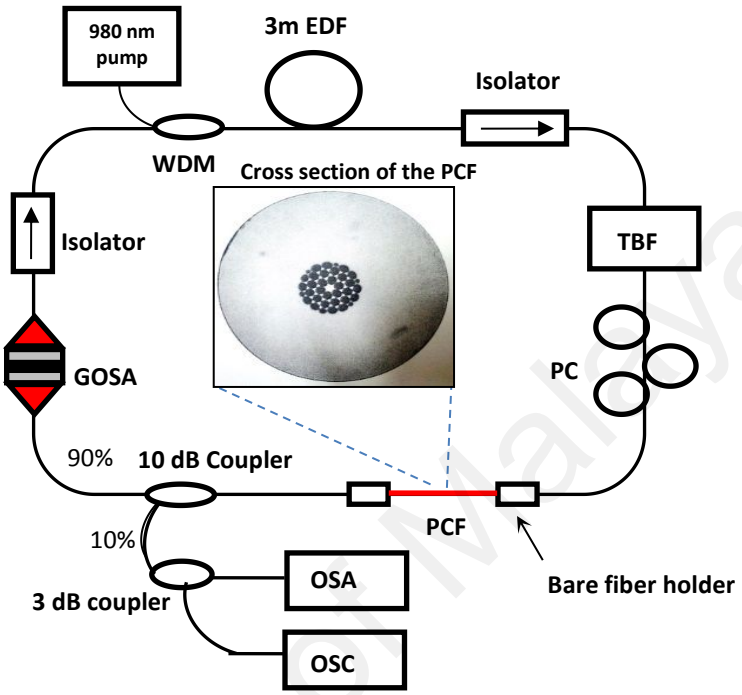

Figure 4.9: Experimental setup of the dual-wavelength Q-switched fiber laser. Inset shows the cross section of the PCF.

At first, the generation of the dual-wavelength fiber laser (DWFL) was obtained by pumping a 66 mW of 980 nm laser from the laser diode into the ring cavity without the GOSA. The optical spectrum of the narrow spacing DWFL was monitor using a high resolution OSA (APEX AP2051A – with highest resolution of 0.16 pm at a span of 0.164 nm). The PC is fine tune until dual-wavelength laser is generated and measured from the OSA as shown in Figure 4.10 (a), where the spacing between the two wavelengths of 28 pm is obtained with signal to noise ratio (SNR) of 53.7 dB and 3 dB line width of about 0.6 pm. After the generation of DWFL with stable output observed, the GOSA assembly is then employed into the ring laser cavity to trigger the Q-switching effect. Figure 4.10 (b) shows the optical spectrum scan after the GOSA is

placed in the cavity. Series of spikes are observed due to the large fluctuation of the optical power at high frequency while the OSA scanning through each of the wavelength. The Q-switched DWFL obtained, has an approximately wavelength spacing of 33 pm and a SNR of 49.6 dB, which differs slightly when operating in CW regime due to the change in the laser polarization state when the GOSA assembly is inserted.

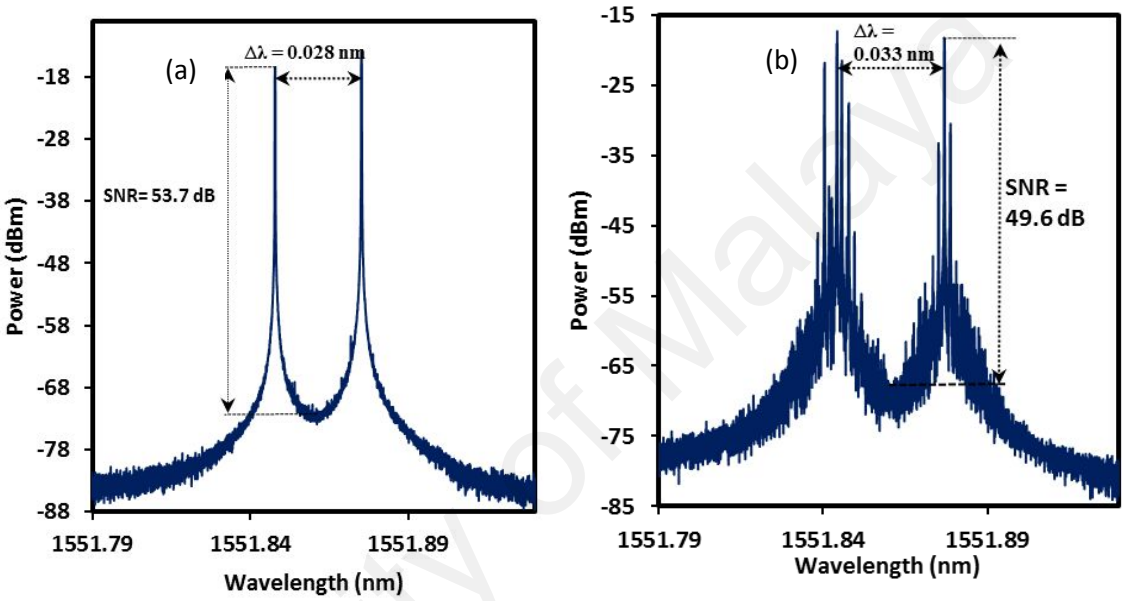

Figure 4.10: Dual-wavelength laser spectra captured using high resolution optical spectrum analyzer at (a) CW and (b) Q-switching with GOSA assembly is employed in the laser cavity.

Figure 4.11 shows the typical pulse train of the Q-switched DWFL at the pump power of 66 mW. It shows a series of stable pulse train with pulse repetition rate of 27.7 kHz and pulse width of around 7.4 μs at full width half maximum (FWHM). The stability of the Q-switched pulses is then analyzed by measuring the power output fluctuation with RFSA. Figure 12 shows the first harmonic RF spectrum of the Q-switched DWFL at 20 kHz span, with resolution and video bandwidth of 300 Hz and 1 MHz respectively. The signal has a peak-to-noise ratio of about 37 dB which confirm pulse stability.

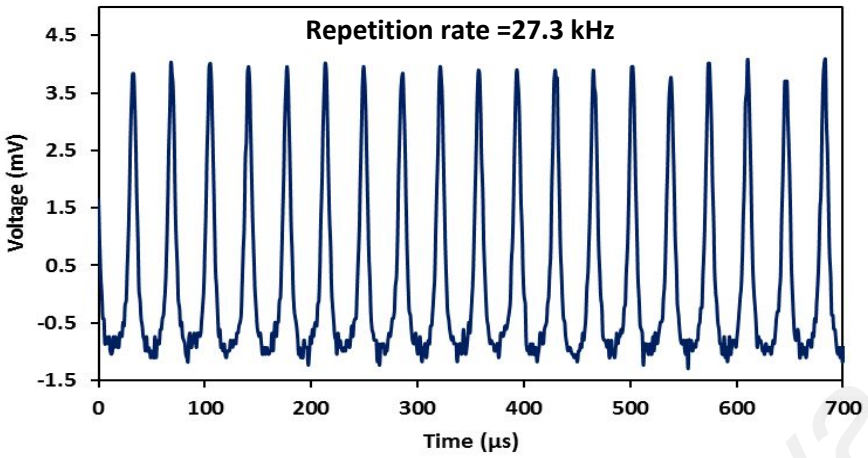

Figure 4.11: Pulse train of the dual-wavelength Q-switched EDFL pumped at 66 mW.

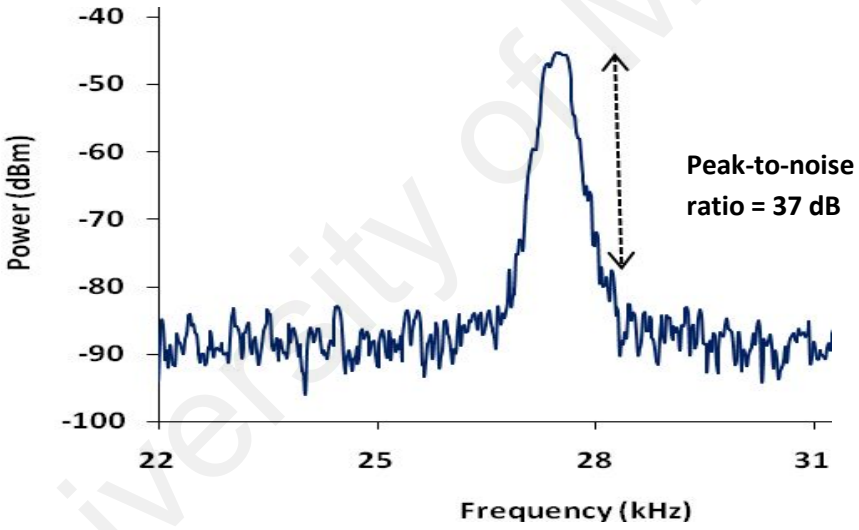

Figure 4.12: First harmonic radio frequency spectrum of the Q-switched DWFL.

The proposed dual-wavelength Q-switched EDFL offers slight tuning in the repetition rate and pulse width to fulfill different applications which need different pulse specifications. The tuning can be performed by changing the 980 nm pump power. Figure 13 shows repetition rate and pulse width curves at different pump powers. The threshold to trigger the Q-switching is level at about 54 mW. The repetition rate increases linearly from the threshold to a maximum repetition rate of 31 kHz at the

pump power of 69 mW. In contrast, the pulse width decreases with exponent manner from 13.2 μs, reaching to a saturation value of about 7.04 μs at 69 mW pump power. However, further increase in pump power leads to pulse instability and broadening. Since the dual-wavelength laser has a very narrow spacing and broad laser spectrum, the two wavelengths will eventually bound to merge together as the pump power is increased. This contributed to unstable dual-wavelength laser generation which limits the further increase of the pump power for Q-switching operation. Figure 4.14 shows the average output power and the calculated pulse energy curves at different pump powers. Both output power and pulse energy increase linearly as the pump power is increased. Under the pump power of 69 mW, the average output power of 0.086 mW and pulse energy of 2.8 nJ are obtained.

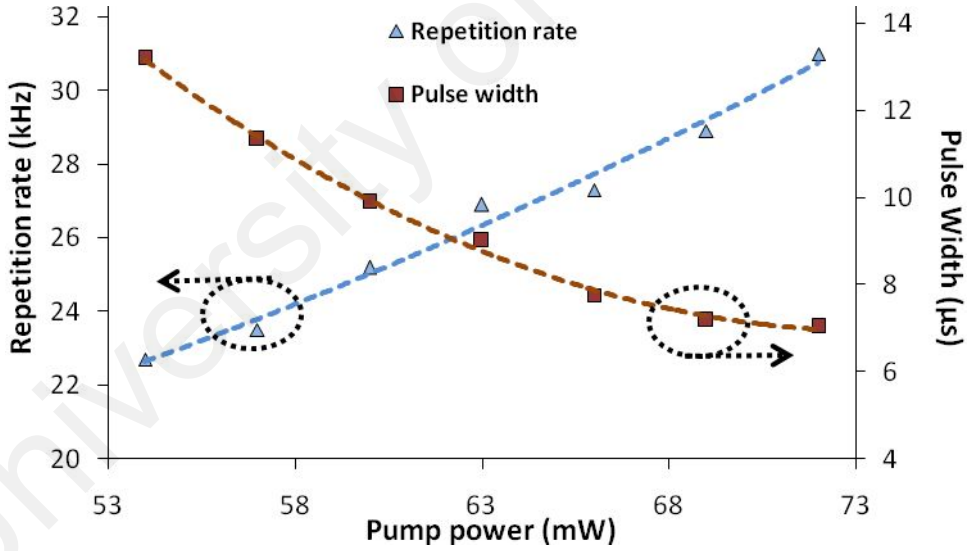

Figure 4.13: Repetition rate and pulse width curves at different pump powers

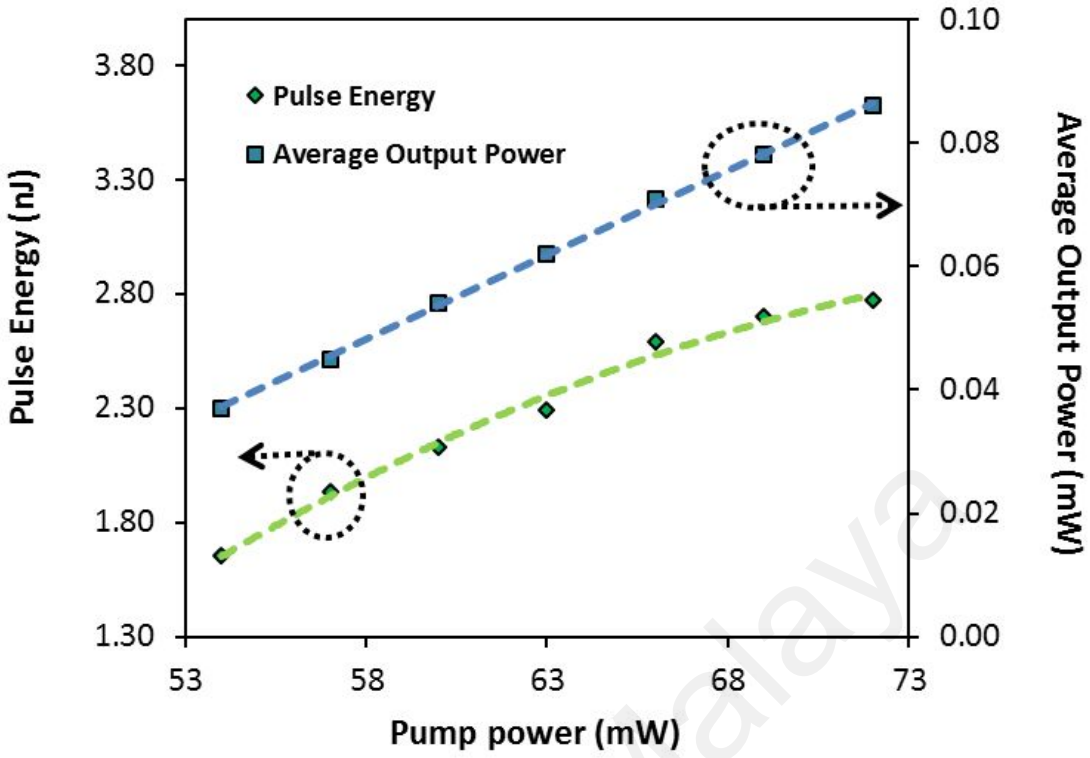

Figure 4.14: Pulse energy and average output power curves at different pump powers.

4.5 Mode-locked EDFL with GO paper as a SA

In the previous two sections, Q-switched EDFLs have been demonstrated using the GO paper based SA. Numerous works have also been reported on graphene based mode-locked fiber lasers in literatures (X. Liu, 2011; Ugolotti et al., 2012; Xu et al., 2012). Recently, Xu. et. al. (Xu et al., 2012) has demonstrated a mode-locked femtosecond EDFLs using GOSA. The SA was prepared by immersing a broadband mirror into a graphene oxide hydrosol. After 48 hour, a thin graphene membrane was formed on top of the broadband reflective mirror. In another work, Sobon *et al.* (Sobon et al., 2012) compares the performances of graphene oxide and reduced graphene oxide as SA. The saturable absorbers were placed on fused silica substrate and inserted between two collimating gradient index (GRIN) lenses to achieve mode-locked fiber lasers. In this section, we demonstrate a femtosecond mode-locked EDFL using the GO

paper as a mode-locker. The paper is sandwiched between two fiber ferrules to initiate mode-locking in proposed new configuration, which produces soliton pulse train with 15.62 MHz repetition rate and 680 fs pulse width. We observed that the fiber laser has low pulsing threshold as well as low damage threshold. Therefore, pulse energy and peak power are 0.0085 nJ and 11.85 W respectively. The easy fabrication of GO paper will promote its potential in ultrafast photonics applications.

The schematic of the proposed mode-locked EDFL is shown in Figure 4.15. It was constructed using a simple ring cavity, in which a 1.6 m long EDF was used instead of 0.8 m or 3 m EDF for Q-switching application. The EDF was forward pumped by a 1480 nm laser diode via a 1480/1550 nm WDM. The polarization independent isolator was used to ensure unidirectional light propagation in the cavity and thus facilitate self-starting laser. The total length of the laser cavity was measured to be approximately 12.6 meter, comprising 1.6 m EDF and 11 meter SMF-28 fiber. The Group Velocity Dispersion (GVD) for the EDF and SMF-28 were -21.64 ps/nm/km and 17 ps/nm/km respectively at 1550 nm. Therefore, the resultant total GVD for this mode-locked fiber laser was estimated to be 0.1513 ps/nm/km. This indicated that the proposed mode-locked fiber laser operated in the anomalous dispersion regime and thus it could be classified as a soliton fiber laser. The laser output was obtained via a 95/5 output coupler located between the isolator and SA, which channeled out about 5% of the oscillating light from the ring cavity. All components used in our setup were polarization independent, i.e. they support any light polarization. No PC was included in the laser cavity as we had observed earlier that a PC did not improve our pulse stability. There was no significant pulse jitter observed through the oscilloscope during the experiment.

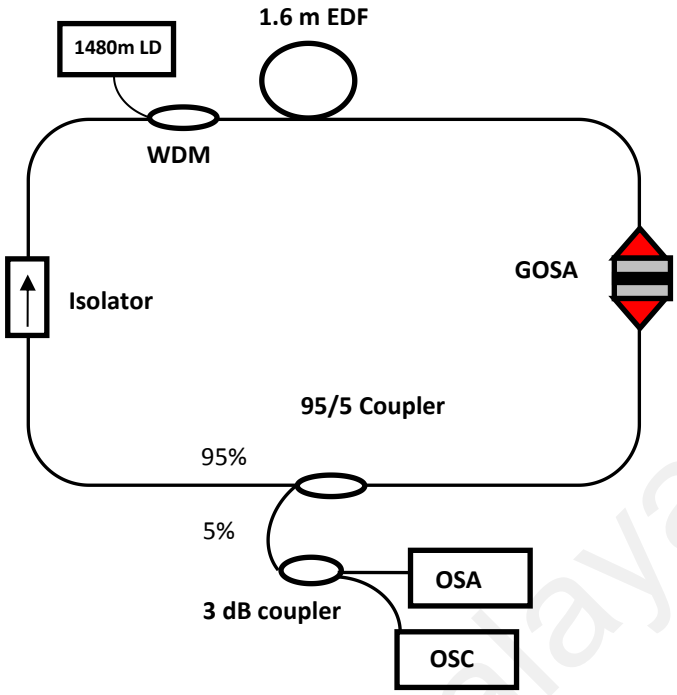

Figure 4.15: The configuration of the proposed mode-locked EDFL

The mode-locked fiber laser had a low self-starting threshold; approximately at 8.7 mW. Figure 4.16 shows the spectral profile where the presence of soliton is confirmed. The solitons' central wavelength, λc, is situated at 1567.9 nm and the 3-dB bandwidth is approximately 7.44 nm with strong Kelly side bands at 1559.3 nm and 1576.1 nm. The spectrum is free from CW parasitic lasing. The presence of Kelly side bands confirms that this mode-lock fiber laser is operating in anomalous dispersion regime. Figure 4.17 shows the typical pulse train of the passive mode-locked fiber laser obtained at pump power of 18 mW. It has a cavity round trip time of 64.1 ns, corresponding to a pulse repetition rate 15.6 MHz and a cavity length of 12.6 m.

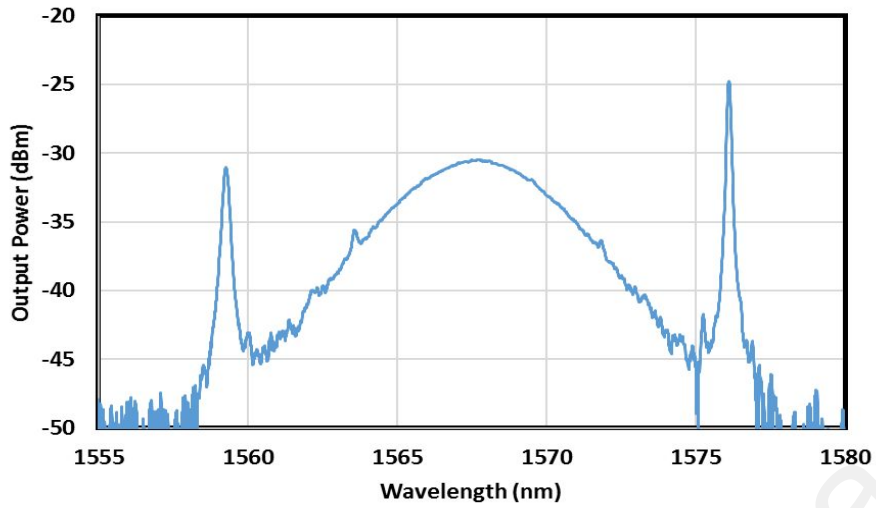

Figure 4.16: Output spectrum of the mode-locked EDFL. Inset shows the typical pulse train at pump power of 18 mW.

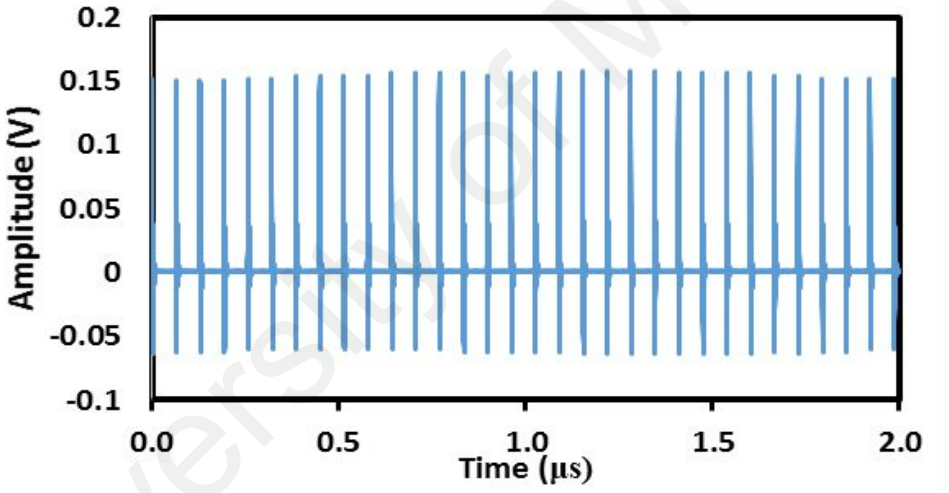

Figure 4.17: Typical pulse train of the GO paper based mode-locked EDFL

Figure 4.18 shows the second harmonic generation (SHG) auto correlation trace, with the estimated pulse duration of 870 fs at its full-width half maximum (FWHM). The sech² fitting which indicates the generation of the soliton pulse is also included in the figure. The auto correlation trace reveals that the experimental result follows the sech² fitting closely. Figure 4.19 shows the RF spectrum of the soliton mode-locked EDFL at repetition rate of 15.6 MHz. It shows a signal to noise ratio of about 70 dB, which indicates the stability of the output pulse train. A time-bandwidth product (TBP)

is calculated to be about 0.78 from the 3-dB bandwidth of the optical spectrum. This shows that the pulse is a chirped pulse. Since the pulsing threshold is low, the output power for this fiber laser is 0.061 mW. Consequently, the resultant pulse energy and peak power are 3.9 pJ and 4.2 W respectively.

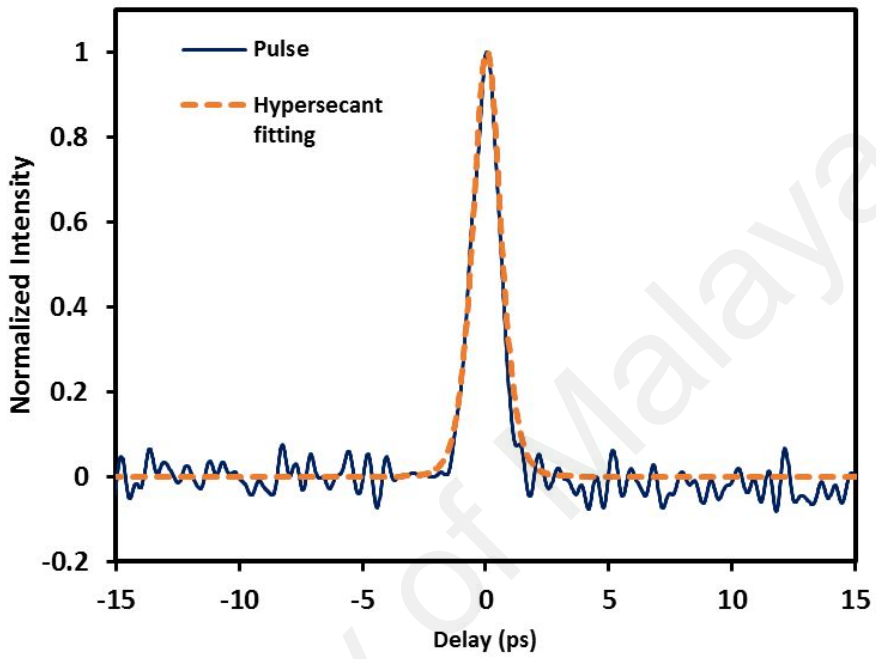

Figure 4.18: The SHG auto correlation trace of the mode-locked laser. Inset shows the RF spectrum.

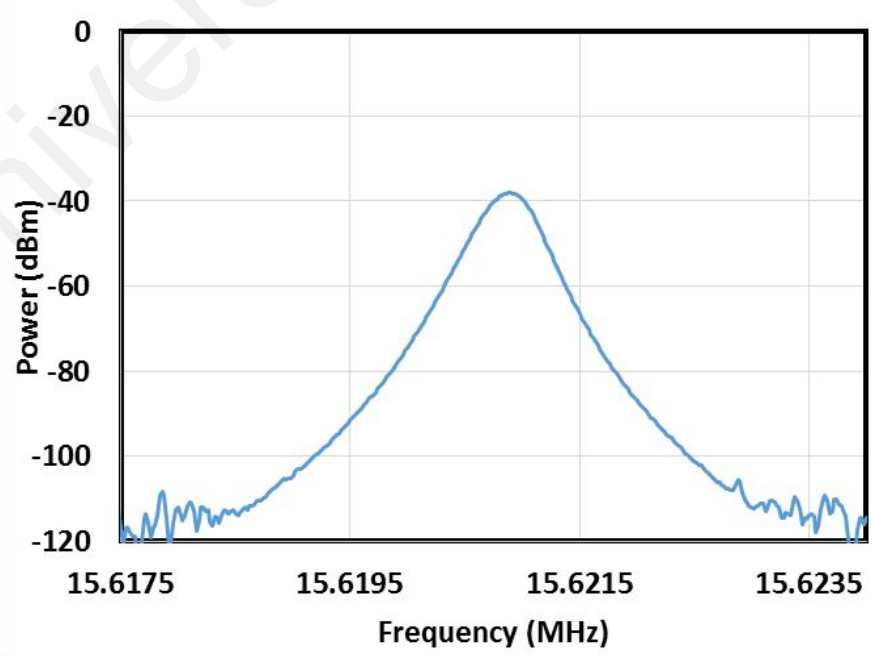

Figure 4.19: RF spectrum of the soliton mode-locked EDFL

4.6 Summary

We have successfully demonstrated Q-switched and mode-locked EDFLs by using a commercial non conductive GO paper as saturable absorber (SA). The paper is sandwiched between two fiber ferrules and incorporated into the laser cavity for pulse generation. A Q-switching pulse train was achieved at 1534.4 nm by using a 0.8 m long EDF as gain medium in a ring configuration. The pulse repetition rate changes from 14.3 to 31.5 kHz while the corresponding pulse width decreases from 32.8 to 13.8 μs as the 980 nm pump power is increased from the Q-switching threshold value of 22.0 to 50.5 mW. A narrow spacing Q-switched DWFL is also demonstrated using the GOSA. It employ PCF and a TBF in the setup to produce a dual-wavelength laser output with a wavelength spacing of 33 pm and a SNR of around 49.6 dB. The DWFL can operate at a maximum repetition rate of 31 kHz, with its pulse duration of 7.04 μs and pulse energy of 2.8 nJ. We have also successfully demonstrated a soliton mode-locked fiber laser by using a GOSA in a ring cavity comprising of a 1.6 m long EDF, which was pumped by a 1480 nm laser diode. The laser generates a pulse train with a repetition rate of 15.62 MHz, pulse width of 870 fs, pulse energy 3.9 pJ and peak power of 4.2 W. The SA has a relatively low self-starting threshold although susceptible to damage at higher pump power. The SA is only able to withstand pulse operation for a short period of time. Given by the simplicity of preparing a GO paper, these experiments prove that a non conductive GO paper can be an alternative to existing graphene and GO based SA.

CHAPTER 5

CONCLUSION AND FUTURE OUTLOOK

The field of fiber lasers and fiber optic devices has experienced a sustained rapid growth despite witnessing the infamous 'telecom bubble burst'. All-fiber optic devices have inherent advantages of relatively low cost, compact design, light weight, low maintenance, and increased vibration tolerances. One of the important fiber-optic devices is pulse laser, which has a broad range of applications ranging from industry to optical communication. In this MPhil research, various new pulsed fiber lasers operating in single-wavelength and dual-wavelength modes are proposed and demonstrated using a low cost and simple approach. In this final chapter, we will conclude what has been demonstrated and the future outlook will be discussed. The following are highlights of the achievements of this thesis with details to follow;

Development of Q-switched fiber lasers based on NPR

Q-switching is a technique that enables the generation of a short optical pulse by sudden switching of the cavity Q factor, i.e., of the cavity loss. Compared to CW fiber lasers, high-peak-power Q-switched Erbium-doped fiber lasers (EDFLs) are practically useful in numerous applications, such as optical communications, light detection and ranging (lidar), differential absorption lidar, and as pumps for mid-IR generation. Q-switched fiber lasers can be realized by many different physical mechanisms depending on pulse duration, energy and repetition rate. Currently, Semiconductor Saturable Absorber Mirrors (SESAMs) which is a real saturable is the dominant passive saturable

absorber and are commercially available in the market. SESAMs require complex fabrication as they are typically fabricated by molecular beam epitaxy (MBE) and usually require post-growth processing in order to reduce their response time. SESAMs also have a limited operation range (typically limited to a few tens of nanometers). This limitation motivates researchers to find new materials to construct SA or new technique for pulse generation.

In this work, we experimentally demonstrate a stable passive Q-switched fiber laser operating at 1543.5 nm using a double clad Erbium-Ytterbium co-doped fiber (EYDF) as the gain medium in conjunction with nonlinear polarization rotation (NPR) technique. An isolator is used in conjunction with a highly nonlinear EYDF to induce intensity dependent loss in a sufficiently-high loss ring cavity to achieve Q-switched operation with a low pump threshold of 300 mW. At 980 nm multi-mode pump power of 500 mW, the EYDF laser (EYDFL) generates an optical pulse train with a repetition rate of 46.95 kHz, pulse width of 5.3 μs and pulse energy of 75.6 nJ.

Demonstration of dual-wavelength Q-switched fiber lasers based on NPR

We report a room temperature all-fiber dual-wavelength EYDFL operating at 1543.3 nm and 1545.4 nm using a nonlinear polarization rotation technique. An isolator is employed in conjunction with a multi-lobed double-clad Erbium Ytterbium co-doped fiber (EYDF) to induce intensity dependent loss in a sufficiently-high loss ring cavity to achieve dual-wavelength and Q-switching simultaneous operations. At the threshold pump power of 0.27 W, the EYDFL generates a sequence of pulses with repetition rate of 12.06 kHz and pulse width of 11.56 μs. When the multi-mode pump is increased to 0.60 W, the repetition rate can be tuned to 57.94 kHz. The lowest pulse width of 5.04 μs and the maximum pulse energy of 72.01 nJ are obtained at the pump power of 0.55 W. The simple and inexpensive dual-wavelength Q-switched NPR-based laser has a big

potential for applications in metrology, environmental sensing and biomedical diagnostics.

Demonstration of single-wavelength and dual wavelength Q-switched laser using a GO paper saturable absorber

NPR technique was demonstrated earlier for Q-switching applications in 1.5 μm region. However, it strongly depends on the polarization and phase evolution of the optical pulse in the laser cavity, so in a long cavity it can be easily overdriven and affected by the environmentally induced fiber birefringence. This limitation motivates researchers to find new materials such as carbon nanotubes (CNTs) and graphene to construct SA. Both CNTs and graphene have advantages because their excellent recovery time and saturable absorption. As a result of gapless linear dispersion of Dirac electrons, graphene SA is preferable because it can achieve wideband, tunable operation without the need of bandgap engineering or chirality/diameter control as in CNTs. However, the processability is the first issue for the graphene based materials. Recently, the interest on GO is increasing because its synthesis is relatively easier than graphene. It can be prepared in large quantities in both water and organic solvents. A graphene oxide paper has also been developed and commercially available for various applications. In this work, two different Q-switched Erbium-doped fiber lasers (EDFLs) are demonstrated using a commercially available graphene oxide (GO) paper as a saturable absorber (SA). The SA is constructed by sandwiching the GO paper between two fiber connectors. A stable and self-starting Q-switched operation was achieved at 1534.4 nm by using a 0.8 m long Erbium-doped fiber (EDF) as gain medium. The pulse repetition rate changes from 14.3 to 31.5 kHz while the corresponding pulse width decreases from 32.8 to 13.8 μs as the pump power is increased from 22.0 to 50.5 mW. A narrow spacing dual-wavelength Q-switched EDFL can also be realized by including

a photonics crystal fiber and a tunable Bragg filter in the setup. It can operate at a maximum repetition rate of 31 kHz, with its pulse duration of 7.04 μs and pulse energy of 2.8 nJ. These results show that the proposed GO paper is a suitable SA component for generating both single wavelength and multi-wavelength Q-switched laser in the 1.5 micron wavelength region.

Demonstration of a mode-locked fiber laser using a GO paper saturable absorber

Passively mode-locked EDFLs have been extensively investigated because of their compactness, flexibility, and low cost. They can be realized using various mode locking techniques including nonlinear optical loop mirror (NOLM), NPR and various saturable absorbers (SAs). In this work, mode-locked EDFL was demonstrated by using non conductive GO paper as saturable absorber (SA). A GO SA based mode-locked EDFL can be realized by using a 1.6 m long EDF in conjunction with 1480 nm pumping. The laser generates a soliton pulse train with a repetition rate of 15.62 MHz and pulse width of 870 fs. It is observed that the proposed fiber lasers have a low pulsing threshold pump power as well as low damage threshold. The easy fabrication of GOSA should promote its potential application in laser photonics.

Much work has been carried out on the generation of Q-switched and mode-locked EDFL based on both a passive SA and NPR technique. However, it can be further explored and investigated in the future especially on the improving the lasing characteristic and ultra-short pulse generation. The proposed Q-switched and mode-locked fiber laser can also be tailored to operate in the new wavelength regions such as 1.0 and 2.0 micron using Ytterbium and Thulium fiber, respectively as the gain medium. With the advancement of ultrafast laser system, the cavity length can also be reduced to

several meters to allow hundreds of Mega-Hertz and also Giga-Hertz repetition rate for applications in high capacity telecommunication systems and photonic switching devices. Future works should focus on improving fabrication of the saturable absorbers and optimizing of laser cavity to improve the quality of output pulse train.

REFERENCES

Ado, J., Dresselhaus, M., Ricchiro, S., & Dresselhaus, G. (2011). Raman Spectroscopy in Graphene Related Systems: Wiley-VCH Verlag, Germany.

Ahmad, F., Harun, S., Nor, R., Zulkepely, N., Ahmad, H., & Shum, P. (2013). A passively mode-locked erbium-doped fiber laser based on a single-wall carbon nanotube polymer. *Chinese Physics Letters, 30*(5), 054210.

Anyi, C., Haris, H., Harun, S. W., Ali, N. M., & Arof, H. (2013). Nanosecond pulse fibre laser based on nonlinear polarisation rotation effect. *Electronics Letters, 49*(19), 1240-1241.

Armitage, J. R. (1988). Three-level fiber laser amplifier: a theoretical model. *Applied optics, 27*(23), 4831-4836.

Becker, P. M., Olsson, A. A., & Simpson, J. R. (1999). *Erbium-doped fiber amplifiers: fundamentals and technology*: Academic press.

Bonaccorso, F., Sun, Z., Hasan, T., & Ferrari, A. (2010). Graphene photonics and optoelectronics. *Nature photonics, 4*(9), 611-622.

Chang, Y. M., Lee, J., Jhon, Y. M., & Lee, J. H. (2011). Active Q-switching in an erbium-doped fiber laser using an ultrafast silicon-based variable optical attenuator. *Optics express, 19*(27), 26911-26916.

Chang, Y. M., Lee, J., & Lee, J. H. (2012). Active mode-locking of an erbium-doped fiber laser using an ultrafast silicon-based variable optical attenuator. *Japanese Journal of Applied Physics, 51*(7R), 072701.

Digonnet, M. J. (2002). *Rare-Earth-Doped Fiber Lasers and Amplifiers, Revised and Expanded*: CRC press.

Digonnet, M. J., Liu, K., & Shaw, H. J. (1990). Characterization and optimization of the gain in Nd-doped single-mode fibers. *Quantum Electronics, IEEE Journal of, 26*(6), 1105-1110.

Dikin, D. A., Stankovich, S., Zimney, E. J., Piner, R. D., Dommett, G. H., Evmenenko, G., . . . Ruoff, R. S. (2007). Preparation and characterization of graphene oxide paper. *Nature, 448*(7152), 457-460.

Dong, X., Su, C.-Y., Zhang, W., Zhao, J., Ling, Q., Huang, W., . . . Li, L.-J. (2010). Ultra-large single-layer graphene obtained from solution chemical reduction and its electrical properties. *Physical Chemistry Chemical Physics, 12*(9), 2164-2169.

El-Sherif, A. F., & King, T. A. (2003). High-energy, high-brightness Q-switched Tm 3+-doped fiber laser using an electro-optic modulator. *Optics communications, 218*(4), 337-344.

Etzel, H., Gandy, H., & Ginther, R. (1962). Stimulated emission of infrared radiation from ytterbium activated silicate glass. *Appl. Optics, 1*.

Fan, Y.-X., Lu, F.-Y., Hu, S.-L., Lu, K.-C., Wang, H.-J., Dong, X.-Y., . . . Wang, H.-T. (2004). Tunable high-peak-power, high-energy hybrid Q-switched double-clad fiber laser. *Optics letters, 29*(7), 724-726.

Feng, C., Liu, D., & Liu, J. (2012). Graphene oxide saturable absorber on golden reflective film for Tm: YAP Q-switched mode-locking laser at 2 μm. *Journal of Modern Optics, 59*(21), 1825-1828.

Ferrari, A. C., & Robertson, J. (2000). Interpretation of Raman spectra of disordered and amorphous carbon. *Physical review B, 61*(20), 14095.

Hamzah, A., Paul, M. C., Awang, N., Ahmad, H., Pal, M., Das, S., . . . Harun, S. (2013). Passively mode-locked erbium doped zirconia fiber laser using a nonlinear polarisation rotation technique. *Optics & Laser Technology, 47*, 22-25.

Hanna, D., Jauncey, I., Percival, R., Perry, I., Smart, R., Suni, P., . . . Tropper, A. (1988). Continuous-wave oscillation of a monomode thulium-doped fibre laser. *Electronics letters, 24*(19), 1222-1223.

Hanna, D., Percival, R., Smart, R., Townsend, J., & Tropper, A. (1989). Continuous-wave oscillation of holmium-doped silica fibre laser. *Electronics Letters, 25*(9), 593-594.

Harun, S., Ismail, M., Ahmad, F., Ismail, M., Nor, R., Zulkepely, N., & Ahmad, H. (2012). A Q-switched erbium-doped fiber laser with a carbon nanotube based saturable absorber. *Chinese Physics Letters, 29*(11), 114202.

He, X., Liu, Z.-B., Wang, D., Yang, M., Liao, C., & Zhao, X. (2012). Passively mode-locked fiber laser based on reduced graphene oxide on microfiber for ultra-wide-band doublet pulse generation. *Journal of Lightwave Technology, 30*(7), 984-989.

Huang, J., Huang, W., Zhuang, W., Su, K., Chen, Y., & Huang, K. (2009). High-pulse-energy, passively Q-switched Yb-doped fiber laser with AlGaInAs quantum wells as a saturable absorber. *Optics letters, 34*(15), 2360-2362.

Huang, N., Lim, H., Chia, C., Yarmo, M., & Muhamad, M. (2011). Simple room-temperature preparation of high-yield large-area graphene oxide. *International journal of nanomedicine, 6*, 3443.

Kao, K., & Hockham, G. A. (1966). *Dielectric-fibre surface waveguides for optical frequencies*. Paper presented at the Proceedings of the Institution of Electrical Engineers.

Kapany, N. (1967). Fiber optics. Principles and applications. *New York: Academic Press, 1967, 1*.

Kapron, F., Keck, D. B., & Maurer, R. D. (1970). Radiation losses in glass optical waveguides. *Applied Physics Letters, 17*(10), 423-425.

Keller, U. (2003). Recent developments in compact ultrafast lasers. *Nature, 424*(6950), 831-838.

Kobtsev, S., Kukarin, S., & Fedotov, Y. (2008). High-energy Q-switched fiber laser based on the side-pumped active fiber. *Laser Physics, 18*(11), 1230-1233.

Koester, C. J., & Snitzer, E. (1964). Amplification in a fiber laser. *Applied Optics, 3*(10), 1182-1186.

Lin, J. H., Lin, K.-H., Hsu, C., Yang, W., & Hsieh, W. F. (2007). Supercontinuum generation in a microstructured optical fiber by picosecond self Q-switched mode-locked Nd: GdVO4 laser. *Laser Physics Letters, 4*(6), 413.

Liu, P., Hou, J., Zhang, B., Chen, S., & Chen, J. (2012). Passively mode-locked fiber ring laser using semiconductor saturable absorber mirror. *Laser Physics, 22*(1), 273-277.

Liu, X. (2011). Interaction and motion of solitons in passively-mode-locked fiber lasers. *Physical Review A, 84*(5), 053828.

Loh, K. P., Bao, Q., Eda, G., & Chhowalla, M. (2010). Graphene oxide as a chemically tunable platform for optical applications. *Nature chemistry, 2*(12), 1015-1024.

Luo, Z.-C., Luo, A.-P., Xu, W.-C., Yin, H.-S., Liu, J.-R., Ye, Q., & Fang, Z.-J. (2010). Tunable multiwavelength passively mode-locked fiber ring laser using intracavity birefringence-induced comb filter. *Photonics Journal, IEEE, 2*(4), 571-577.

Luo, Z., Zhou, M., Weng, J., Huang, G., Xu, H., Ye, C., & Cai, Z. (2010). Graphene-based passively Q-switched dual-wavelength erbium-doped fiber laser. *Optics letters, 35*(21), 3709-3711.

Maiman, T. H. (1960). Stimulated optical radiation in ruby.

Martinez, A., & Sun, Z. (2013). Nanotube and graphene saturable absorbers for fibre lasers. *Nature Photonics, 7*(11), 842-845.

Mears, R. J., Reekie, L., Poole, S., & Payne, D. N. (1985). Neodymium-doped silica single-mode fibre lasers. *Electronics Letters, 21*(17), 738-740.

Mears, R. J., Reekie, L., Poole, S., & Payne, D. N. (1986). Low-threshold tunable CW and Q-switched fibre laser operating at 1.55 μm. *Electronics Letters, 22*(3), 159-160.

Miya, T., Terunuma, Y., Hosaka, T., & Miyashita, T. (1979). Ultimate low-loss single-mode fibre at 1.55 μm. *Electronics Letters, 15*(4), 106-108.

Pan, L., Utkin, I., & Fedosejevs, R. (2007). Passively Q-switched ytterbium-doped double-clad fiber laser with a Cr 4+: YAG saturable absorber. *Photonics Technology Letters, IEEE, 19*(24), 1979-1981.

Park, N., Dawson, J. W., Vahala, K. J., & Miller, C. (1991). All fiber, low threshold, widely tunable single-frequency, erbium-doped fiber laser with a widely Fabry–Perot filter. *Applied physics letters, 59*(19), 2369-2371.

Pask, H., Carman, R. J., Hanna, D. C., Tropper, A. C., Mackechnie, C. J., Barber, P. R., & Dawes, J. M. (1995). Ytterbium-doped silica fiber lasers: versatile sources for the 1-1.2 μm region. *Selected Topics in Quantum Electronics, IEEE Journal of, 1*(1), 2-13.

Poole, S., Payne, D. N., & Fermann, M. E. (1985). Fabrication of low-loss optical fibres containing rare-earth ions. *Electronics Letters, 21*(17), 737-738.

Popa, D., Sun, Z., Hasan, T., Torrisi, F., Wang, F., & Ferrari, A. (2010). Graphene Q-switched, tunable fiber laser. *arXiv preprint arXiv:1011.0115*.

Reekie, L., Mears, R. J., Poole, S. B., & Payne, D. N. (1986). Tunable single-mode fiber lasers. *Lightwave Technology, Journal of, 4*(7), 956-960.

Reisfeld, R., & Jørgensen, C. K. (1977). *Lasers and excited states of rare earths*: Springer-Verlag Berlin.

Set, S. Y., Yaguchi, H., Tanaka, Y., & Jablonski, M. (2004). Laser mode locking using a saturable absorber incorporating carbon nanotubes. *Lightwave Technology, Journal of, 22*(1), 51-56.

Snitzer, E. (1961). Proposed fiber cavities for optical masers. *Journal of Applied Physics, 32*(1), 36-39.

Snitzer, E., Po, H., Hakimi, F., Tumminelli, R., & McCollum, B. (1988). *Double clad, offset core Nd fiber laser.* Paper presented at the Optical fiber sensors.

Snitzer, E., & Woodcock, R. (1965). Yb3+–Er3+ GLASS LASER. *Applied Physics Letters, 6*(3), 45-46.

Sobon, G., Sotor, J., Jagiello, J., Kozinski, R., Zdrojek, M., Holdynski, M., . . . Abramski, K. M. (2012). Graphene oxide vs. reduced graphene oxide as saturable absorbers for Er-doped passively mode-locked fiber laser. *Optics express, 20*(17), 19463-19473.

Stone, J., & Burrus, C. (1974). Neodymium-doped fiber lasers: room temperature cw operation with an injection laser pump. *Quantum Electronics, IEEE Journal of, 10*(9), 794-794.geometry. *Applied Physics Letters, 23*(7), 388-389.

Sun, Z., Hasan, T., Torrisi, F., Popa, D., Privitera, G., Wang, F., . . . Ferrari, A. C. (2010). Graphene mode-locked ultrafast laser. *ACS nano, 4*(2), 803-810.

Sun, Z., Rozhin, A., Wang, F., Hasan, T., Popa, D., O'neill, W., & Ferrari, A. (2009). A compact, high power, ultrafast laser mode-locked by carbon nanotubes. *Applied Physics Letters, 95*(25), 253102.

Suni, P. J., Hanna, D. C., Percival, R., Perry, I. R., Smart, R. G., Townsend, J. E., & Tropper, A. C. (1990). *Lasing characteristics of ytterbium, thulium and other rare-earth doped silica based fibers.* Paper presented at the OE/FIBERS'89.

Tausenev, A., Obraztsova, E., Lobach, A., Chernov, A., Konov, V., Kryukov, P., . . . Dianov, E. (2008). 177fs erbium-doped fiber laser mode locked with a cellulose

polymer film containing single-wall carbon nanotubes. *Applied Physics Letters, 92*(17), 171113.

Ugolotti, E., Schmidt, A., Petrov, V., Kim, J. W., Yeom, D.-I., Rotermund, F., . . . Fiebig, C. (2012). Graphene mode-locked femtosecond Yb: KLuW laser. *Applied Physics Letters, 101*(16), 161112.

Wang, H.-Y., Xu, W.-C., Luo, A.-P., Dong, J.-L., Cao, W.-J., & Wang, L.-Y. (2012). Controllable dissipative soliton and Q-switched pulse emission in a normal dispersion fiber laser using SESAM and cavity loss tuning mechanism. *Optics Communications, 285*(7), 1905-1907.

Wang, J., Luo, Z., Zhou, M., Ye, C., Fu, H., Cai, Z., . . . Qi, W. (2012). Evanescent-light deposition of graphene onto tapered fibers for passive Q-switch and mode-locker. *Photonics Journal, IEEE, 4*(5), 1295-1305.

Wang, K., Wang, J., Fan, J., Lotya, M., O'Neill, A., Fox, D., . . . Zhao, Q. (2013). Ultrafast saturable absorption of two-dimensional MoS2 nanosheets. *ACS nano, 7*(10), 9260-9267.

Wang, Q., Chen, T., Zhang, B., Li, M., Lu, Y., & Chen, K. P. (2013). All-fiber passively mode-locked thulium-doped fiber ring laser using optically deposited graphene saturable absorbers. *Applied Physics Letters, 102*(13), 131117.

Wang, Y., & Xu, C.-Q. (2007). Actively Q-switched fiber lasers: Switching dynamics and nonlinear processes. *Progress in Quantum Electronics, 31*(3), 131-216.

Xu, J., Liu, J., Wu, S., Yang, Q.-H., & Wang, P. (2012). Graphene oxide mode-locked femtosecond erbium-doped fiber lasers. *Optics express, 20*(14), 15474-15480.

Zhao, C., Zhang, H., Qi, X., Chen, Y., Wang, Z., Wen, S., & Tang, D. (2012). Ultra-short pulse generation by a topological insulator based saturable absorber. *Applied Physics Letters, 101*(21), 211106.

Zhao, S., Surwade, S. P., Li, Z., & Liu, H. (2012). Photochemical oxidation of CVD-grown single layer graphene. *Nanotechnology, 23*(35), 355703.

Zhu, Y., Murali, S., Cai, W., Li, X., Suk, J. W., Potts, J. R., & Ruoff, R. S. (2010). Graphene and graphene oxide: synthesis, properties, and applications. *Advanced materials, 22*(35), 3906-3924.

LIST OF PULICATIONS

1. Babar, I. M.; Sabran, M. B. S.; Harun, Sulaiman Wadi; et al., "Q-switched thulium-ytterbium co-doped fibre laser using newly developed octagonal shaped inner cladding double-clad active fibre and multi-walled carbon nanotubes passive saturable absorber," IET OPTOELECTRONICS Volume: 9 Issue: 3 Pages: 131-135 Published: JUN 2015.

2. Babar, I. M.; Sabran, M. B. S.; Rahman, A. A.; et al., "Multi-lobed double-clad Erbium-Ytterbium co-doped Q-switched fiber laser based on nonlinear polarisation rotation technique," JOURNAL OF NONLINEAR OPTICAL PHYSICS &MATERIALS Volume: 24 Issue: 1 Article Number: 1550002 Published: MAR 2015.

3. Sabran, M. B. S.; Jusoh, Z.; Babar, I. M.; et al., "DUAL-WAVELENGTH PASSIVELY Q-SWITCHED ERBIUM YTTERBIUM CODOPED FIBER LASER BASED ON A NONLINEAR POLARIZATION ROTATION TECHNIQUE," MICROWAVE AND OPTICAL TECHNOLOGY LETTERS Volume: 57 Issue: 3 Pages: 530-533 Published: MAR 2015.

4. Babar, I. M.; Sabran, M. B. S.; Jusoh, Z.; et al., "Double-clad thulium/ytterbium co-doped octagonal-shaped fibre for fibre laser applications," UKRAINIAN JOURNAL OF PHYSICAL OPTICS Volume: 15 Issue: 4 Pages: 173-183 Published: DEC 2014.

5. Sulaiman Wadi Harun1,2, Muhamad Burhan Shah Sabran1, Salam Mahdi Azooz2, Ahmad Zarif Zulkifli 2, Mohd Afiq Ismail2, Harith Ahmad1, "Q-switching and mode-locking pulse generation with graphene oxide paper-based saturable absorber," The Journal of Engineering; Received on 28th November 2014; Accepted on 17th February 2015, J Eng 2014 doi: 10.1049/joe.2014.0321.